[Papers in Palaeontology, Vol. 5, Part 1, 2019, pp. 47–81]

CHAROPHYTES FROM THE CRETACEOUS–PALEOCENE BOUNDARY IN THE SONGLIAO BASIN (NORTH-EASTERN CHINA): A CHINESE BIOZONATION AND ITS CALIBRATION TO THE GEOMAGNETIC POLARITY TIME SCALE

by SHA LI[1,*], QIFEI WANG[2], HAICHUN ZHANG[3], XIAOQIAO WAN[4] *and* CARLES MARTÍN-CLOSAS[5,*]

[1]CAS Key Laboratory of Economic Stratigraphy & Palaeogeography, Nanjing Institute of Geology & Palaeontology, Centre for Excellence in Life & Paleoenvironment, Chinese Academy of Sciences, 39 East Beijing Road, Nanjing, 210008, China; shali@nigpas.ac.cn
[2]Nanjing Institute of Geology & Palaeontology, Centre for Excellence in Life & Paleoenvironment, Chinese Academy of Sciences, 39 East Beijing Road, Nanjing, 210008, China
[3]State Key Laboratory of Palaeobiology & Stratigraphy, Nanjing Institute of Geology & Palaeontology, Center for Excellence in Life & Paleoenvironment, Chinese Academy of Sciences, 39 East Beijing Road, Nanjing, 210008, China
[4]State Key Laboratory of Biogeology & Environmental Geology, China University of Geosciences, Beijing, 100083, China
[5]Departament de Dinàmica de la Terra i de l'Oceà, Facultat de Ciències de la Terra, Universitat de Barcelona, Barcelona, 08028, Catalonia Spain; cmartinclosas@ub.edu
*Corresponding authors

Typescript received 31 January 2018; accepted in revised form 5 April 2018

Abstract: Charophyte assemblages from the mid-Campanian and lower Paleocene of the SK-1(North) borehole in the Songliao Basin (NE China) are here re-studied. Four charophyte biozones and one superzone are defined in the Sifangtai and Mingshui formations and correlated to the Geomagnetic Polarity Time Scale. These include a mid–late Campanian *Atopochara trivolvis ulanensis* Zone, a latest Campanian – early Maastrichtian *Microchara gobica* Zone, a late Maastrichtian *Microchara prolixa* Zone, and an earliest Danian *Peckichara sinuolata* Zone. The latter three zones are grouped within the *Microchara cristata* Superzone, which allows intra- and intercontinental correlation with other basins in China and Europe. *Peckichara sinuolata* first appears in chron C29r (upper Mingshui Formation) and is proposed as the basal marker of the Paleocene. The biozonation of the K/Pg interval proposed for the Songliao Basin differs from a previous biozonation proposed in the Pingyi Basin since it represents a different biogeographical and palaeoecological context. In the mid-Campanian to Maastrichtian, the flora was limited to freshwater lakes in northern China and Mongolia, whereas in the Pingyi Basin, brackish water dominated. In the Paleocene, the Songliao Basin contained a diverse flora consisting of nine species that thrived in terrigenous and temporary lakes, whereas the flora in the Pingyi Basin was dominated by one species inhabiting permanent alkaline lakes. The species common to the two basins are widely distributed in Eurasia and constitute a useful tool for long-distance correlations, but serve as a less-precise tool for detailed biostratigraphical subdivision within one specific basin.

Key words: charophytes, K/Pg boundary, biozonation, Songliao Basin, palaeoecology.

THE Cretaceous–Palaeogene boundary (K/Pg boundary) is one of the most interesting and controversial boundaries in the geological record, mainly with regard to major mass extinctions. The Global Stratotype Section and Point (GSSP) for the base of the Danian Stage is defined at the base of the boundary clay in a section near El Kef, Tunisia, in open marine facies (Molina *et al.* 2006). However, a similar consensus, even at regional scale, has not been reached for the K/Pg boundary in non-marine settings. This is mainly due to incomplete stratigraphic successions and fossil records, especially in the very conspicuous red beds occurring near the boundary, where fossils are rare. Charophyte biostratigraphy has proved to be a useful tool to address this problem because the calcified fructifications called gyrogonites and utricles persist despite frequent oxidation of these facies, and allow for easy correlation between marine and non-marine records, and even for correlation between different continents.

In China, Upper Cretaceous charophytes are abundant in the Songliao, Pingyi, North Jiangsu, Jianghan and

doi: 10.1002/spp2.1225

Nanxiong basins. Charophytes from the Pingyi Basin were recently studied by Li *et al.* (2016) based on detailed taxonomic and palaeoecological analyses. Charophytes from the North Jiangsu Basin were studied by Wang *et al.* (1982) and Wang (2004), while those from the Nanxiong Basin were studied by Huang (1988). Charophytes from the Jianghan Basin were studied by Wang (1978*a*), Li (1985) and Li *et al.* (2010). The latter authors suggested that the section they studied was one of the most complete K/Pg boundary sections in non-marine facies worldwide, containing abundant charophytes and ostracods. They defined the K/Pg boundary in the Paomagang Formation based on the end-Cretaceous porocharacean *Feistiella anluensis*, a brackish species, and on the early Paleocene occurrence of the characeans *Peckichara huananensis* (formerly *Neochara huananensis*).

The Songliao Basin is the largest basin with a continuous non-marine record from the K/Pg boundary in China. Charophytes from this basin were previously studied by Wang *et al.* (1985). One biozone including three subzones were established in the Sifangtai and Mingshui formations. However, the material studied by Wang *et al.* (1985) from over 100 boreholes was not tightly collected, and gyrogonite intraspecific polymorphism was not taken into account. Furthermore, this biozonation lacked an accompanying palaeoecological analysis, which is a prerequisite for establishing charophyte biozones. Indeed, species with wide ecological requirements are preferred for biostratigraphic correlation (Sanjuan & Martín-Closas 2012; Vicente *et al.* 2015). Recently, Li *et al.* (2013) re-studied the charophytes from the Songliao Basin based on the complete SK-1(North) borehole, but again intraspecific polymorphism was not taken into account, which resulted in an overestimation of the number of taxa identified. For the present study, charophytes from the SK-1(North) borehole were re-sampled with greater precision to improve these weak points. The charophyte assemblages from Songliao are also calibrated to the Geomagnetic Polarity Time Scale (GPTS), based on the magnetostratigraphy of the same borehole proposed by Deng *et al.* (2013). These results are compared with those from other Chinese basins and a new regional biozonation is proposed as a framework for establishing a future Chinese charophyte biozonation of the K/Pg boundary.

MATERIAL AND METHOD

The charophytes described in this study were obtained from a Cretaceous–Paleocene borehole in the Songliao Basin, north-eastern China. In 2007, the National Basic Research Program of China (2006CB701400) conducted a whole-core program in the Songliao Basin, which led to the recovery of a composite core representing almost all of the Upper Cretaceous to Paleocene succession. Two boreholes, SK-1(South) and SK-1(North), were drilled about 75 km apart (Fig. 1), correlated by a marker-layer of lacustrine black shale at the bottom of Member 2 of the Nenjiang Formation, and charophytes were collected from borehole SK-1(North) at coordinates 46°12′44.22″ N, 124°15′56.78″ E.

Charophytes were obtained from siltstones and claystones. The 10 cm diameter core resulting from continuous logging was sampled at an average of 1 m intervals and more than 1100 samples were prepared. The samples were re-sampled for additional material three more times for this study. The first and second fossil preparations were processed in the Laboratory of Micropalaeontology, China University of Geosciences, Beijing, while the third and fourth preparations were processed in the State Key Laboratory of Palaeobiology and Stratigraphy, Nanjing Institute of Geology and Palaeontology, Chinese Academy of Science. One to two hundred grammes of sediment per sample (up to 1000 g in significant beds) dry weight were disaggregated in water for several weeks prior to sieving through two sieves of mesh size 63 and 1140 μm. Gyrogonites were picked out under a binocular microscope. Unclean specimens were subjected to ultrasound, sometimes following prior treatment with the chemical reagent EDTA. Selected gyrogonites were studied and biometrically measured using a Zeiss Stereo Discovery V16 microscope at the State Key Laboratory of Palaeobiology and Stratigraphy, Nanjing. Finally, they were photographed with a scanning electron microscope in the China University of Geosciences, Beijing, and the State Key Laboratory of Palaeobiology and Stratigraphy, Nanjing Institute of Geology and Palaeontology, Chinese Academy of Sciences. The specimens are housed in the palaeobotanical collection (PB22606–PB22675) of the Nanjing Institute of Geology and Palaeontology (NIGPAS), Chinese Academy of Sciences, China.

X-ray microtomography was used in this study to determine the internal structure of the gyrogonite basal plate. The specimen was scanned at the NIGPAS micro-CT laboratory using a Zeiss Xradia 520 versa 3D X-ray microscope, which provides a nondestructive tomographic reconstruction of microfossils at submicron resolution.

Deng *et al.* (2013) studied the magnetostratigraphy of the deposits yielding charophytes, enabling calibration of the charophyte floras. Identification of the magnetochrons is supported by four SIMS 206Pb/238U zircon ages of volcanic layers interbedded with the sedimentary section of the south core (He *et al.* 2012). Combining

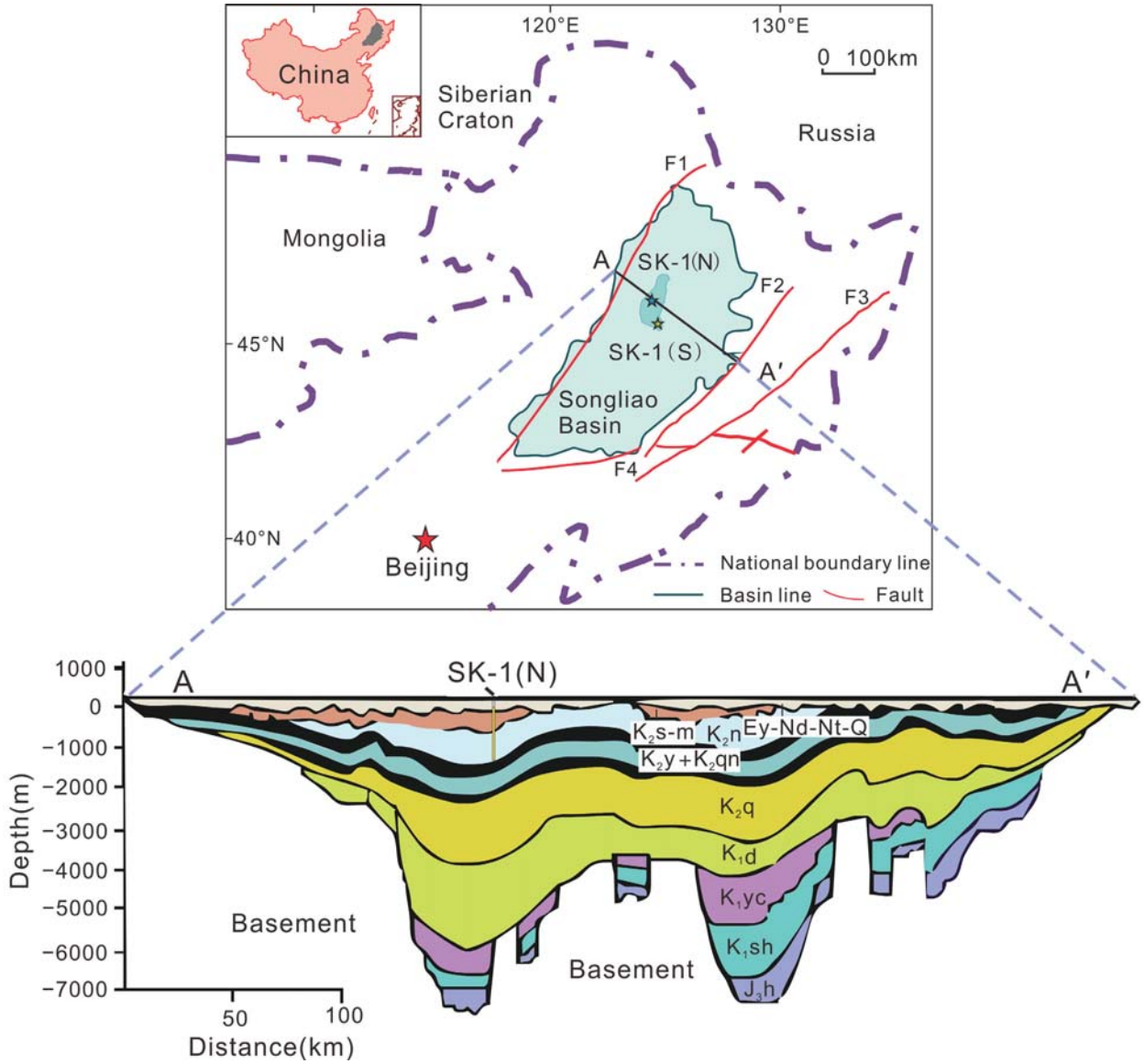

FIG. 1. Location of the SK-1(North) borehole in the Songliao Basin. F1, Nenjiang Fault; F2, Yilan-Yitong Fault; F3, Chifeng-Kaiyuan Fault. A–A′, stratigraphic cross section through the Songliao Basin modified from Wang *et al.* (2007) and Qu *et al.* (2014). J_3, Upper Jurassic; K_1, Lower Cretaceous; K_2, Upper Cretaceous; J_3h, Huoshiling Formation; K_1sh, Shahezi Formation; K_1yc, Yingcheng Formation; K_1d, Denglouku Formation; K_2q, Quantou Formation; K_2qn, Qingshankou Formation; K_2y, Yaojia Formation; K_2n, Nenjiang Formation; K_2s-m, Sifangtai and Mingshui formations; Ey-Nd-Nt-Q, Eocene Yi'an Formation–Neogene Da'an and Taikang formations, Quaternary deposits. Colour online.

lithostratigraphy, U–Pb zircon geochronology, and magnetostratigraphy, polarity intervals C34n to C29r in the GPTS were recognized (Cande & Kent 1995) and compared to the Geologic Time Scale (Gradstein *et al.* 2004). Chron C29r (342.1–317.03 m), including the K/Pg boundary is located in the upper part of the second member of the Mingshui Formation.

Facies control of charophyte species distribution was performed by means of sedimentological, taphonomic and palaeoecological studies. The stratigraphic and sedimentological data have already been published in a number of previous studies (e.g. Cheng *et al.* 2009; Gao *et al.* 2013; Wang *et al.* 2013, 2015). The charophyte taphonomic analysis was conducted herein based on their state of preservation and whether there was an association between different organs from the same plant. Palaeoecological studies were performed by combining sedimentological and taphonomic information and taking into account data from other associated palaeontological remains.

GEOLOGICAL SETTING

The Songliao Basin is located between 119°40′ and 128°24′ E, and 42°25′–49°23′ N, and stretches over 260 000 km^2, roughly encompassing the provinces of Heilongjiang, Jilin and Liaoning in NE China (Fig. 1). The basin trends in a north-north-east direction and the basin floor is diamond-shaped. It is *c.* 820 km long in the north–south direction and *c.* 350 km wide in the east–west direction (Wang *et al.* 1994, 2013).

Stratigraphy

Terrestrial records of the late Mesozoic and early Cenozoic in the Songliao Basin are up to 7000 m thick and comprise volcanic, volcaniclastic and sedimentary rocks that are unevenly distributed across the basin (Gao *et al.* 1994; Wang, *et al.* 2001). The Upper Jurassic and Cretaceous consist of 10 formations. From bottom to top, there are: the Huoshiling Formation (J_3h), Shahezi Formation (K_1sh), Yingcheng Formation (K_1yc), Denglouku Formation (K_1d), Quantou Formation (K_2q), Qingshankou Formation (K_2qn), Yaojia Formation (K_2y), Nenjiang Formation (K_2n), Sifangtai Formation (K_2s) and Mingshui Formation (K_2m). The general lithostratigraphical and palaeontological features of these formations are provided in Table 1. The charophytes studied are from the Sifangtai and Mingshui formations.

Basin evolution

The evolutionary history of the Songliao Basin can be divided into four stages:

1. A pre-rift doming stage during the pre-Late Jurassic (before 155 Ma). Uplift and erosion resulting from mantle doming led to the erosion of the Triassic to Middle Jurassic deposits. Volcanics interbedded with alluvial sediments were well developed (Feng *et al.* 2010).
2. A rift stage during the latest Jurassic–earliest Cretaceous, forming the Huoshiling, Shahezi and Yingcheng formations. Over 30 isolated rift sub-basins were formed and show a record of volcaniclastic deposits interbedded with fluvial, deltaic and lacustrine sediments (Feng *et al.* 2010).
3. A post-rift stage during late Early Cretaceous and Late Cretaceous periods, when lithospheric cooling and extension led to basin subsidence. The Denglouku, Quantou, Qingshankou, Yaojia and Nenjiang formations were deposited during this stage, representing fluvial, deltaic and lacustrine facies interbedded with oil shales (Feng *et al.* 2010; Wang *et al.* 2013).
4. Regional stress became compressive during the latest Cretaceous and earliest Cenozoic. An angular unconformity between the Nenjiang and Sifangtai formations represents the onset of this compressive setting that followed the deposition of the Mingshui Formation, eventually leading to the uplift and erosion of the basin. The sediments during this period were mainly composed of fluvial and lacustrine deposits.

SYSTEMATIC PALAEONTOLOGY

Division CHAROPHYTA Migula, 1897
Class CHAROPHYCEAE Smith, 1938
Order CHARALES Lindley, 1836
Family CLAVATORACEAE Pia, 1927
Subfamily ATOPOCHAROIDEAE Peck, 1938

Genus ATOPOCHARA Peck, 1938 emend. Peck, 1941
Atopochara trivolvis ulanensis (Kyansep-Romaschkina, 1975) Martín-Closas & Wang, 2008
Figures 2A–C, 3

1975 *Atopochara ulanensis* Kyansep-Romaschkina, pp. 190–191, pl. 2 fig. 2a–b, pl. 3 figs 1–2.
2008 *Atopochara trivolvis ulanensis* comb. nov.; Martín-Closas & Wang, p. 445.

Material. More than 100 utricles per sample were collected from samples obtained at the depths of 859.54 and 855.61 m respectively. Less abundant gyrogonites were obtained from 13 samples at other depths in the borehole studied (Fig. 4).

Description. The utricle is 759–1093 μm high (mean: 926 μm) and 764–1039 μm wide (mean: 902 μm). It is composed of three equivalent units; each unit is composed of three branches. The left and central branches include three bract-cells, two of them very elongated, while the third, right bract is roughly quadrangular. The right branch is divided into two small and roughly triangular bracts. The right bract of each branch originates near the basal pore and ends near the equator. The left and middle bracts of the left and middle branches turn clockwise to the apex. Apex is round or conical, with a round pore, about 116 μm in diameter. Base is round, with a round pore, 83–100 μm in diameter. Gyrogonites not calcified and the cast of the oospore within the utricle displays a well-developed apical neck and basal column.

Distribution. The lineage of *Atopochara trivolvis* was first described by Grambast (1967, 1968) as belonging to the *Perimneste–Atopochara* lineage and was later considered by Martín-Closas (1989, 1996) and Schudack (1993) as a succession of gradualistic forms within one single evolutionary species. Its biogeographical history has been described by Martín-Closas & Wang (2008). In the

TABLE 1. Lithostratigraphical descriptions of formations in the Songliao Basin.

Age	Formation	Thickness (m)	Lithological description	Fossils
Cretaceous–Palaeogene	Mingshui	Up to 576	Distributed only in the central and western parts of the basin. It is composed of grey-green, grey, black and brown-red shale and grey-green sandstone, related to fluvial and lacustrine facies (Feng *et al.* 2010).	Bivalves, gastropods, ostracods, charophytes
Cretaceous	Sifangtai	Up to 320	Distributed throughout the basin; its main thickness is developed in the central area. It mainly consists in conglomerates, grey and red sandstones, and green and red siltstone and claystones, related to fluvial and lacustrine facies.	Bivalves, gastropods, ostracods, charophytes
	Nenjiang	100–470	Represented throughout the whole basin. It is formed by grey to dark limestones and marls, and grey fine sandstones and mudstones interbedded with oil shales, corresponding to lacustrine facies (Feng *et al.* 2010; Wang *et al.* 2013).	Ostracods, vascular plant fossils, charophytes
	Yaojia	80–210	Distributed across the basin. It is composed of red, green, grey and dark siltstones and mudstones interbedded with oil shales related to deltaic, fluvial and lacustrine facies (Feng *et al.* 2010; Wang *et al.* 2013).	Ostracods, charophytes
	Qingshankou	260–500	Distributed across the basin except in its western part. It composed of grey and dark mudstones interbedded with oil shales and sandstones, corresponding to deltaic and lacustrine facies (Feng *et al.* 2010; Wang *et al.* 2013).	Ostracods, vascular plant fossils, charophytes
	Quantou	550–1200	Mainly distributed in the central and eastern part of the basin but represented across it. It is formed by conglomerates at the base overlain by red, purple and brown mudstones intercalated with conglomerates and sandstones of fluvial origin, including braided and meandering river facies as well as lacustrine deposits (Feng *et al.* 2010; Wang *et al.* 2013).	Ostracods, plant macroremains, charophytes, spores and pollen
	Denglouku	500–1000	Mainly distributed in the central and eastern parts of the basin. It comprises conglomerates at the base followed by interlayers of dark mudstones and white sandstones (Feng *et al.* 2010; Wang *et al.* 2013). Alluvial plain deposits are distributed along the basin margin while deltaic and lacustrine facies were deposited in the basin centre (Feng *et al.* 2010).	Charophytes
	Yingcheng	500–1000	Widespread across the basin. It is composed of volcanic rocks interbedded with conglomerates, sandstones and several discontinuous coal beds (Feng *et al.* 2010; Wang *et al.* 2013). Alluvial fans and fan deltas are developed close to faults while lacustrine deposits are distributed away from them (Feng *et al.* 2010).	
	Shahezi	400–1500	Its distribution is restricted to fault blocks in the eastern and central rift belts of the basin. It includes a thin layer of tuff and conglomerates at the base but the main thickness comprises mainly fluvio-lacustrine grey to black siltstones and mudstones intercalated with sandstones (Feng *et al.* 2010; Wang *et al.* 2013).	Spores and pollen
Jurassic	Huoshiling	500–1600	Distributed in most fault blocks of the basin. It is composed of volcanic rocks interbedded with fluvial siltstones and claystones and swamp and mire coal deposits (Feng *et al.* 2010; Wang *et al.* 2013).	Plant macroremains, spores and pollen

Campanian to Maastrichtian, *A. trivolvis ulanensis* was the last representative of this lineage worldwide. It occurred in Mongolia and northern China, including the Songliao Basin and the Erlian Basin in Inner Mongolia (Kyansep-Romaschkina 1975; Van Itterbeeck *et al.* 2005).

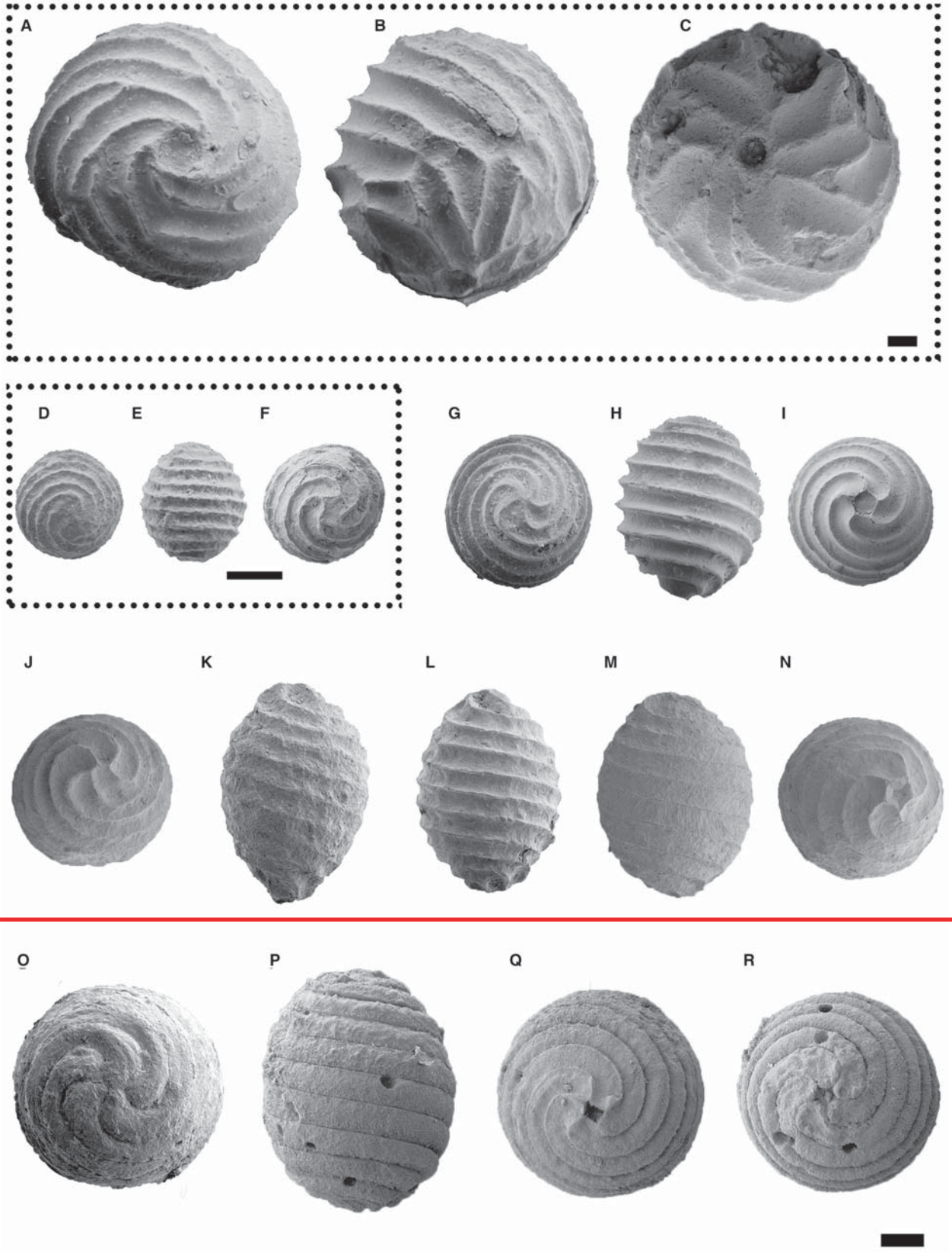
A
B
C
D
E
F
G
H
I
J
K
L
M
N
O
P
Q
R

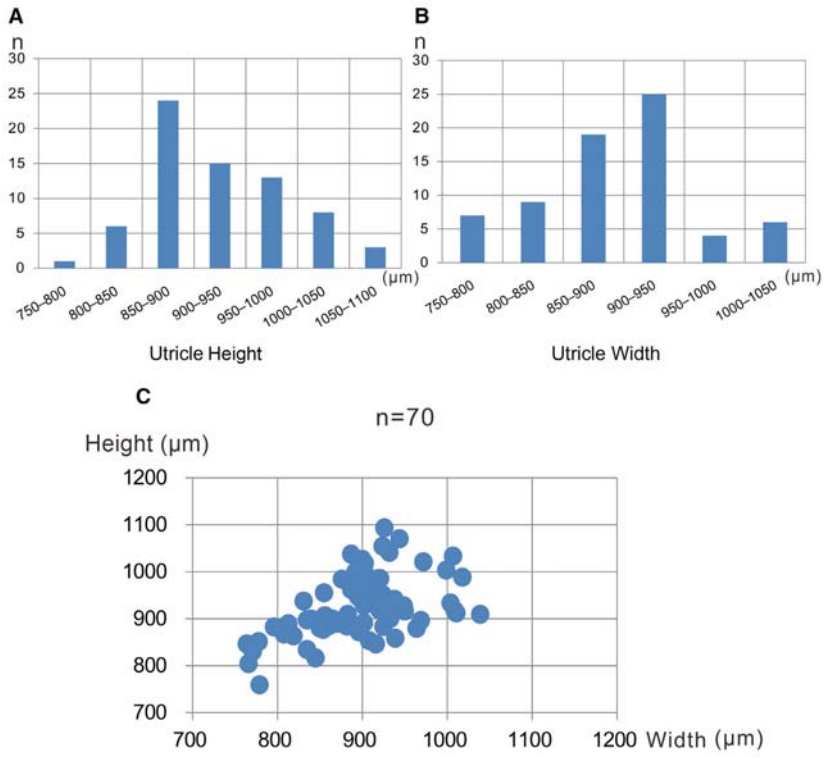

FIG. 3. Biometric data of *Atopochara trivolvis ulanensis* (70 utricles from the depth of 855.61 m) from the SK-1(North) borehole, Songliao Basin. A, height. B, width. C, dispersion graph of the height/width. Colour online.

Family CHARACEAE Agardh, 1824
Subfamily NITELLOIDEAE Braun in Migula, 1897

Genus SPHAEROCHARA (Mädler, 1952) Soulié-Märsche, 1989
Sphaerochara parvula (Reid & Groves, 1921) Horn af Rantzien, 1959
Figures 2D–F, 5

1921 *Tolypella parvula* Reid & Groves, p. 188, pl. 6, figs 4–5.
1959 *Sphaerochara parvula* comb. nov.; Horn af Rantzien, p. 136, pl. 16 figs 10–13.

Material. Small populations with up to 10 gyrogonites occurred in 12 samples at different depths in the borehole studied (Fig. 4).

Description. Gyrogonites very small in size, 261–314 μm high (mean: 288 μm) and 197–272 μm wide (mean: 235 μm). Isopolarity index ranges from 114 to 142, prolate sphaeroidal to subprolate in shape; 9–10 convolutions are visible in lateral view. Spiral cells concave, 22–25 μm wide, without ornamentations or apical modifications. Apex is rounded. Base is rounded with a pentagonal basal plate visible from the exterior, 35–45 μm in diameter.

Remarks. Sphaerochara parvula is characterized by the very small size of the gyrogonite and its large basal plate.

Distribution. The species was first reported in the upper Eocene deposits of the Headon Hill Formation at Hordle cliff, Hampshire, England (Reid & Groves 1921). It was subsequently found in Eocene to Oligocene deposits in Germany (Schwarz 1997 and references therein) and in many other coeval European localities (Riveline 1986). In China, it occurs in Upper Cretaceous to Paleocene deposits in the Jianghan Basin, Hubei Province (Wang 1978*a, b*; Li *et al.* 2010), Hengyang and Dongting basins, Hunan Province (Hu & Zeng 1982, 1983), Nanxiong Basin, Guangdong Province (Huang 1988), and Songliao Basin, North-East China (Li *et al.* 2013). It is also represented in the Cretaceous to Eocene in the Xining-Minhe Basin (Hao *et al.* 1983) and the Eocene in the North Jiangsu Basin, Jiangsu Province (Wang *et al.* 1982; Wang 2004).

FIG. 2. Charophytes from the Songliao Basin. A–C, *Atopochara trivolvis ulanensis*: A, apical view, PB22606; B, lateral view, PB22607; C, basal view, PB22608; sample depth: A–B, 859.54 m; C, 855.61 m. D–F, *Sphaerochara parvula*: D, apical view, PB22609; E, lateral view, PB22610; F, basal view, PB22611; sample depth: 330.37 m. G–I, *Sphaerochara jacobii*: G, apical view, PB22612; H, lateral view, PB22613; I, basal view, PB22614; sample depth: 330.37 m. J–N, *Mesochara biacuta*: J, apical view, PB22615; K–M, lateral views, PB22616–PB22618; N, basal view, PB22619; sample depth: 813.57 m. O–R, *Mesochara* aff. *stantoni*: O, apical view, PB22620; P, lateral view, PB22621; Q–R, basal view, PB22622–PB22623; sample depth, 317.03 m. Scale bars represent 100 μm (A–C; D–F; G–R).

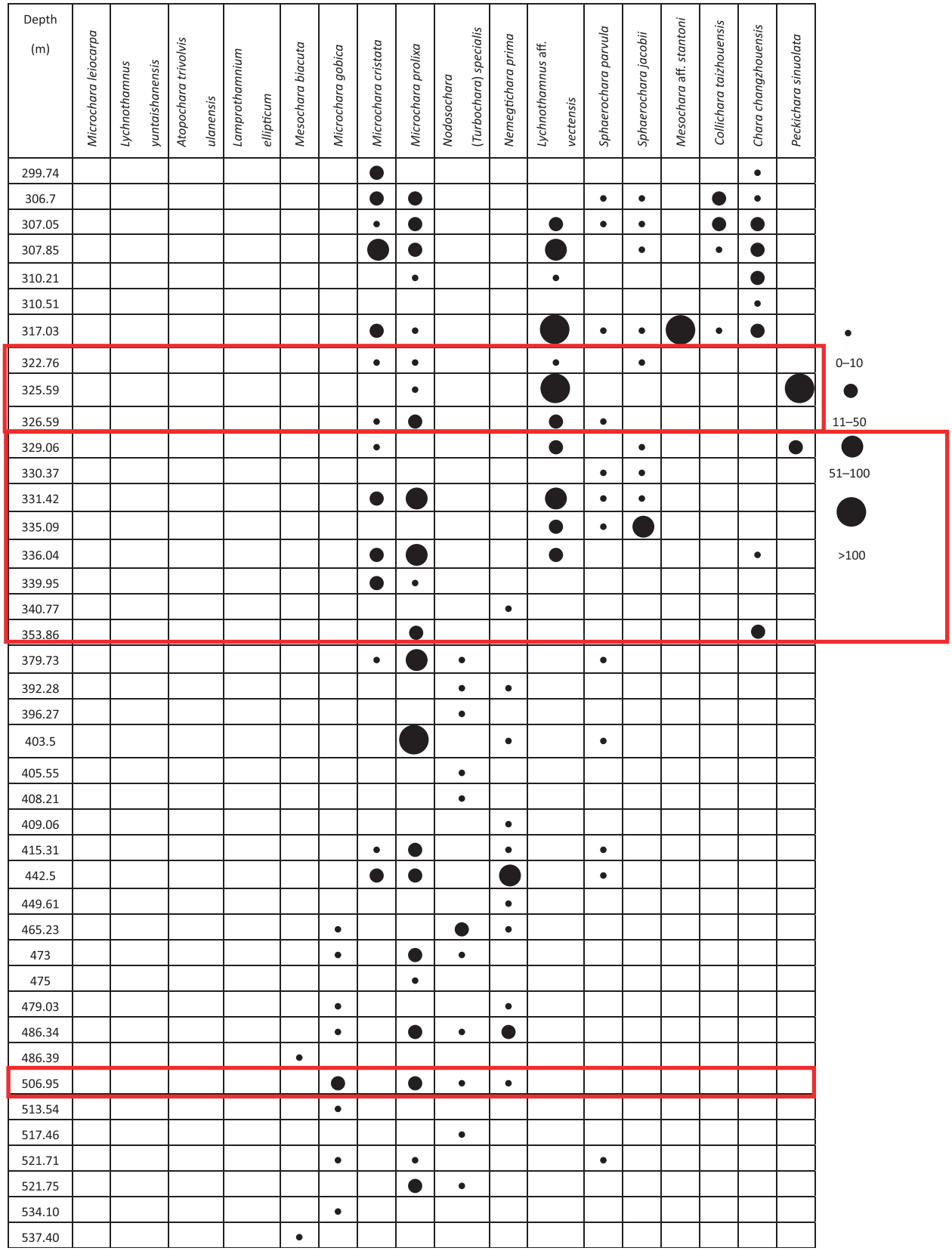

FIG. 4. Abundance of charophyte species from the SK-1(North) borehole in the Songliao Basin.

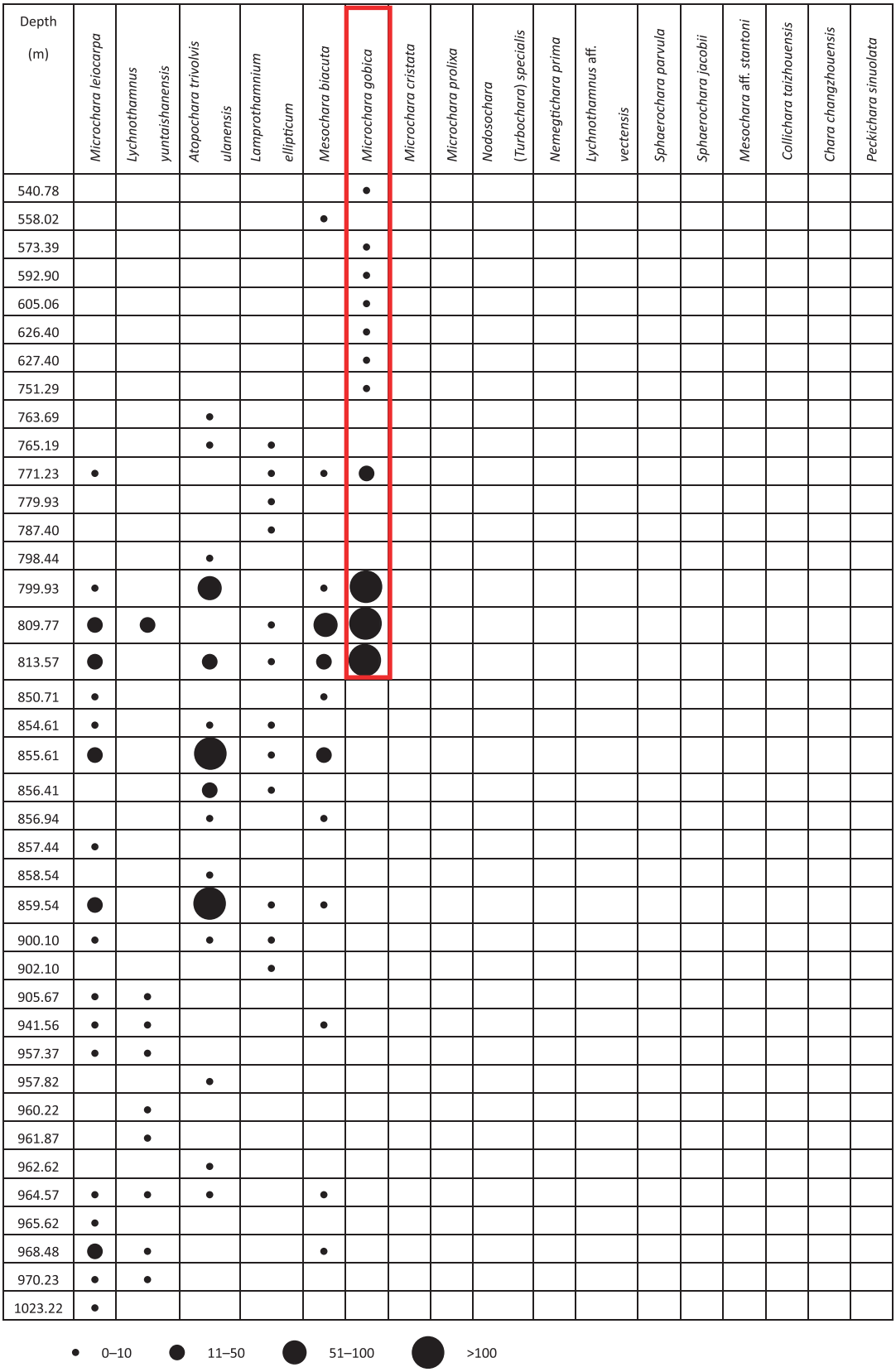

FIG. 4. Continued

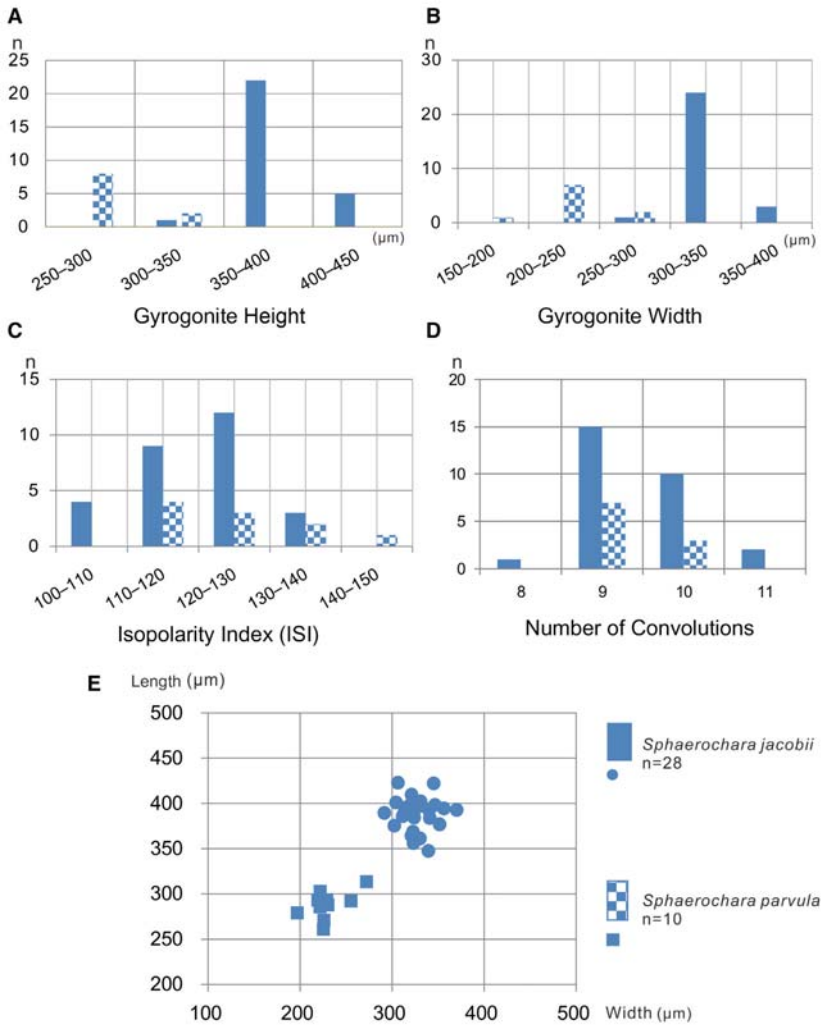

FIG. 5. Biometric data of *Sphaerochara parvula* (10 gyrogonites measured from the depth of 331.42 m) and *Sphaerochara jacobii* (28 from the depth of 335.09 m) from the SK-1(North) borehole, Songliao Basin. A, height. B, width. C, number of convolutions. D, isopolarity index (ISI; height × 100/width). E, dispersion graph of height/width. Colour online.

Sphaerochara jacobii Karczewska & Ziembińska-Tworzydło, 1981

Figures 2G–I, 5

1981 *Sphaerochara jacobii* Karczewska & Ziembińska-Tworzydło, pl. 35 figs 1–3, 7.

Material. 74 gyrogonites were obtained from the depth of 335.09 m. Smaller populations occurred in eight samples from other depths in the borehole studied (Fig. 4).

Description. Gyrogonites are small in size, 347–423 μm high (mean: 385 μm) and 292–370 μm wide (mean: 331 μm). Isopolarity index ranges from 102 to 138, prolate sphaeroidal and subprolate in shape; 8–11 convolutions are visible in lateral view. Spiral cells concave, 50–60 μm wide, without ornamentation. Apex is rounded to prominent. Base is rounded with a pentagonal basal plate visible from the exterior, 45–55 μm in diameter.

Remarks. Sphaerochara jacobii differs from *Sphaerochara parvula* mainly in the larger size of its gyrogonite.

Distribution. This species was first reported in the Upper Cretaceous Nemegt Formation in the Nemegt Basin, Gobi Desert, Mongolia (Karczewska & Ziembińska-Tworzydło 1981). It was subsequently found in the Upper Cretaceous – Paleocene Mingshui Formation in the Songliao Basin, north-east China (Wang *et al.* 1985; Li *et al.* 2013).

Subfamily CHAROIDEAE Braun *in* Migula, 1897

Genus MESOCHARA Grambast, 1962

Mesochara biacuta (Koch & Blissenbach, 1960) Wang *et al.*, 1985

Figures 2J–N, 6

1960 *Tolypella biacuta* Koch & Blissenbach, p. 71, pl. 1 fig. 8, text–fig. 15.

1969 *Mesochara mongolica* comb. nov.; Karczewska & Ziembińska-Tworzydło, p. 132, pl. 30 fig. 1, pl. 34 fig. 1, text–fig. 5.

1985 *Mesochara biacuta* comb. nov.; Wang *et al.*, p. 39, pl. 12 figs 6–8, pl. 13 figs 1–5.

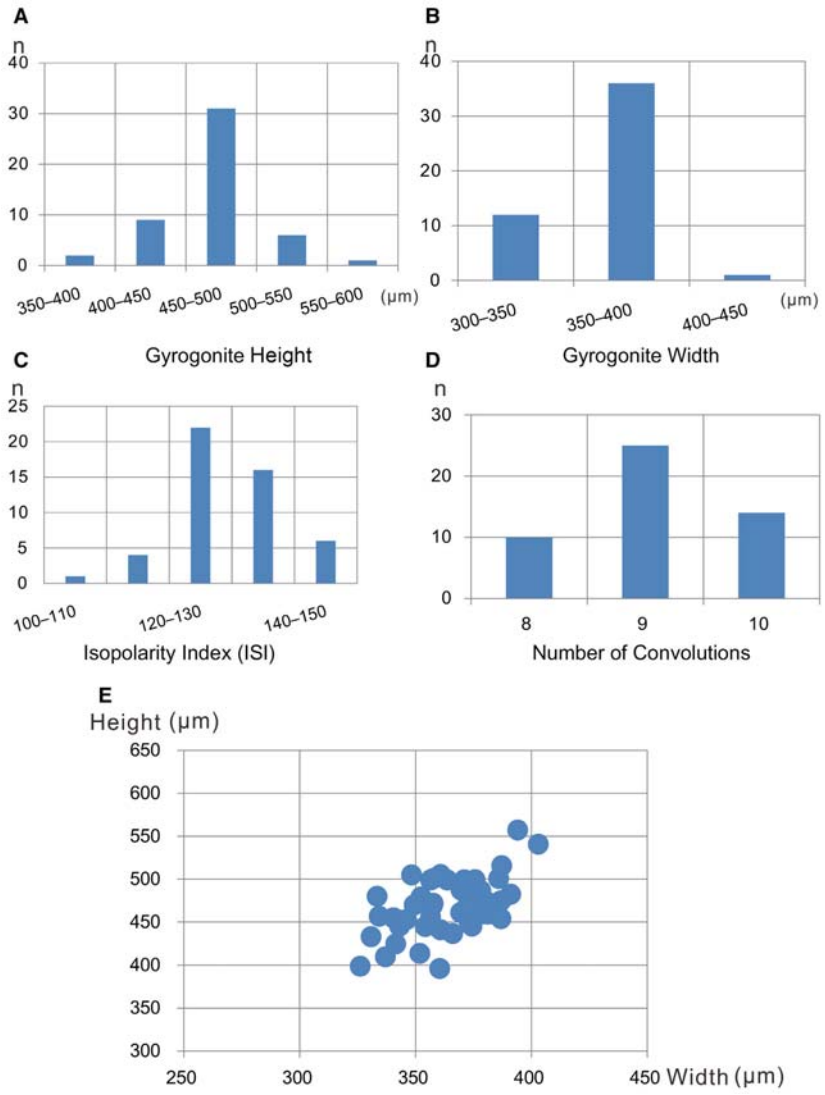

FIG. 6. Biometric data of *Mesochara biacuta* (49 gyrogonites from the depth of 813.57 m) in the SK-1 (North) borehole, Songliao Basin. A, height. B, width; C, isopolarity index (ISI). D, number of convolutions. E, dispersion graph of height/width. Colour online.

Material. About 50 gyrogonites per sample were obtained at the depths 813.57 and 809.77 m. Smaller populations occurred in 12 samples at different depths in the borehole studied (Fig. 4).

Description. Gyrogonites small to medium in size, 396–557 μm high (mean: 477 μm) and 326–403 μm wide (mean: 365 μm). Isopolarity index ranges from 110 to 145, subprolate to prolate in shape; 8–10 convolutions are visible in lateral view. Spiral cells are concave, 40–55 μm in size, and devoid of ornamentation. Apex is round to pointed and does not show any periapical modification. The base is tapering to pointed and displays a pentagonal basal pore, 25–35 μm in size. Basal plate was not observed but is known to be unicellular in this genus (Schudack 1993).

Remarks. Wang *et al.* (1985) reassigned *Tolypella biacuta* Koch & Blissenbach, 1960 to *Mesochara biacuta* based on the shape of the apex and base. However, they did not provide any information about the basal plate, which is still unknown in this particular species. In the population as a whole, specimens displaying pointing apexes and bases typical of *M. biacuta* (Fig. 2K) account for only 10%, the rest showing a more rounded apex (Fig. 2M). There are also intermediate specimens between these morphotypes, which display a slightly pointed apex (Fig. 2L). *Mesochara mongolica* was synonymized with *Mesochara biacuta* by Wang *et al.* (1985) because of its similar morphology.

Distribution. This species was first reported in the Upper Cretaceous of Peru (Koch & Blissenbach 1960). It was later reported in the Upper Cretaceous of the Nemegt Basin in Mongolia (Karczewska & Ziembińska-Tworzydło 1969), the Songliao Basin in China (Wang *et al.* 1985) and the Junggar Basin in Xinjiang (Yang *et al.* 2008).

Mesochara aff. *stantoni* (Knowlton, 1893) Grambast, 1962
Figures 2O–R, 7

1893 *Chara stantoni* Knowlton, p. 141, figs 1–3.
1957 *Sphaerochara stantoni* comb. nov.; Peck, pl. 7 figs 17–21.
1962 *Mesochara stantoni* comb. nov.; Grambast, p. 78.

Material. More than 100 gyrogonites from one sample at a depth of 317.03 m and 99 of them were measured (Fig. 4).

Description. Gyrogonites are medium in size, 480–615 μm high (mean: 548 μm) and 369–494 μm wide (mean: 432 μm). Isopolarity index ranges from 109 to 147, gyrogonite prolate spheroidal and subprolate in shape; 9–13 convolutions are visible in lateral view. Spiral cells convex, 60–70 μm wide, without ornamentation or modifications in the apical zone. Occasionally a well-marked germination suture occurs in the periapical area of specimens. Base is rounded and displays a small, generally pentagonal or star-shaped basal pore, 40–50 μm in diameter.

Remarks. Mesochara aff. *stantoni* from Songliao is characterized by few or no modifications in the apical zone. It cannot be classified within the genus *Sphaerochara* because of its small pentagonal or star-shaped basal pore, with the basal plate not visible from the exterior. This species is different from *Mesochara symmetrica* in being more spheroidal. The material studied is relatively larger than the type *M. stantoni* (510 μm high and 470 μm wide, according to Peck 1957) which also displays concave spiral cells and is older in age (Albian).

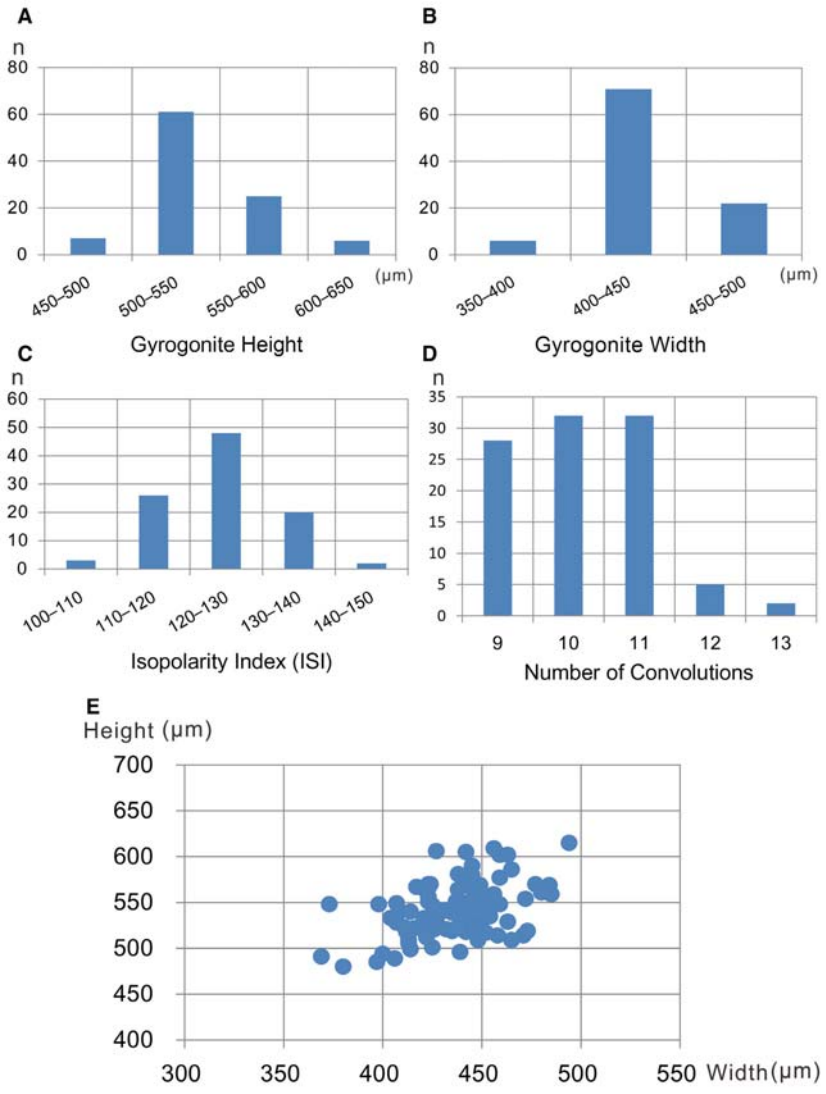

FIG. 7. Biometric data of *Mesochara* aff. *stantoni* (99 gyrogonites measured from the depth of 317.03 m) in the SK-1(North) borehole, Songliao Basin. A, height. B, width. C, isopolarity index (ISI). D, number of convolutions. E, dispersion graph of height/width. Colour online.

Genus MICROCHARA Grambast, 1959
Microchara gobica (Karczewska & Ziembińska-Tworzydło, 1969) comb. nov.
Figures 8A–G, 9

1969 *Tectochara gobica* Karczewska & Ziembińska-Tworzydło, pp. 10, 137–139; pl. 33 figs 1–2; pl. 34 fig. 5.
1975 *Mongolichara costulata*; Kyansep-Romaschkina, p. 202, pl. 5 fig. 3, pl. 6 figs 1, 4.
1979 *Mongolichara gobica* comb. nov.; Karczewska & Kyansep-Romaschkina, p. 424, pl. 3 figs 1–4.
1985 *Raskyaechara gobica* comb. nov.; Wang *et al.*, p. 34, pl. 9 figs 3–8, pl. 10 fig. 1.
1985 *Raskyaechara gobica* var. *songliaoensis* var. nov.; Wang *et al.*, p. 34, pl. 10 figs 2–8.
1985 *Raskyaechara costulata* comb. nov.; Wang *et al.*, p. 36, pl. 11 figs 5–6.

Material. Samples at the depths of 813.57, 809.77 and 799.93 m provided more than 100 gyrogonites each. Smaller populations occurred in 16 samples at different depths in the borehole studied (Fig. 4).

Description. Gyrogonites medium in size, 443–584 μm high (mean: 514 μm) and 357–515 μm wide (mean: 436 μm). Isopolarity index ranges from 103 to 143, prolate spheroidal to subprolate in shape; 7–9 (often 8–9) convolutions are visible in lateral view, 80–100 μm in height. Spiral cells are concave to planar, ornamented with a continuous mid-cellular crest, parallel to sutures. The mid-cellular crest is about the same size or a little wider than the width of sutures (Fig. 8E, F). It disappears in the apex periphery (Fig. 8A) but is continuous to the base (Fig. 8D), reaching the basal pore. Apex is flat to round, without periapical modifications and especially without nodules. Base is round, with a pentagonal basal pore, 40–50 μm in diameter. Basal plate is undivided, in the shape of a pentagonal pyramid (Fig. 8G).

Remarks. This species was first described as *Tectochara gobica* in Mongolia. Karczewska & Ziembińska-Tworzydło (1969) noted that it was distinguished from all other recorded species of *Tectochara* by the strongly developed mid-cellular crest. However, the gyrogonites of this species lack the characteristic periapical thinning and narrowing of the genus *Tectochara*. Later, Karczewska & Kyansep-Romaschkina (1979) reassigned *Tectochara gobica* within *Mongolichara* as *Mongolichara gobica*. They concluded that *Mongolichara deplanata* Kyansep-Romaschkina, 1975 was a junior synonym of *M. gobica* (Karczewska & Kyansep-Romaschkina 1979). Furthermore, they stated that *Mongolichara* also included *M. costulata* Kyansep-Romaschkina, 1975, and *M. aurea* Karczewska & Ziembińska-Tworzydło, 1969 (Karczewska & Kyansep-Romaschkina 1979). Based on the samples from the Songliao Basin, Wang *et al.* (1985) combined *Mongolichara gobica*, *M. deplanata*, and *M. costulata* within the genus *Raskyaechara*, and established the new variety *Raskyaechara gobica* var. *songliaoensis*. This genus was characterized on the basis of a flat and thin apex (when seen in thin section), indicating the absence of a mid-cellular crest in the apical area. All of these taxa except *Raskyaechara deplanata* have been found in the present samples, and the main differences between them lie in different widths of the mid-cellular crests (*Raskyaechara gobica* and *R. costulata*) or in small differences in gyrogonite size (*R. gobica* var. *songliaoensis* is smaller). In the populations studied, transitional morphotypes occurred between the morphotypes representing these taxa, leading us to consider them synonyms.

Compared with *Microchara cristata*, *M. gobica* does not display apical nodules. However, a few of the *M. gobica* gyrogonites studied show a thickening of the spiral cells in the apical centre. This slight thickening is very different from the prominent, comma-shaped nodules of *M. cristata*. Additionally, *M. gobica* never displays a basal column. It also differs from *M. cristata* in its basal plate, which has the shape of a truncated pentagonal pyramid (Fig. 8G) instead of being thin and pentagonal.

Distribution. Mongolichara gobica was first reported from the Nemegt Formation (Upper Cretaceous) in the Nemegt Basin, Gobi Desert, Mongolia (Karczewska & Ziembińska-Tworzydło 1969). It was subsequently found in the Sifangtai and Mingshui formations in the Songliao Basin (Wang *et al.* 1985) and the Honglishan and Hongshaquan formations in the Junggar Basin, Xinjiang Uygur Autonomous Region (Yang *et al.* 2008).

Microchara cristata Grambast, 1971
Figures 8H–M, 10

1971 *Microchara cristata* Grambast, pp. 35–36, figs 22–23, pl. 28 figs 1–8, pl. 29 figs 1–10.
1972 *Gobichara deserta* Karczewska & Ziembińska-Tworzydło, pp. 73–75, figs 10–11, pl. 15 figs 1–5, pl. 16 figs 1–6, pl. 19 fig. 1.
1972 *Gobichara nigra* Karczewska & Ziembińska-Tworzydło, pp. 75–77, fig. 13, pl. 8 figs 3–4, pl. 12 figs 2–5, pl. 13 figs 1–7, pl. 14 figs 2–4, pl. 18 fig. 4.
1972 *Gobichara rubra* Karczewska & Ziembińska-Tworzydło, pp. 77–78, pl. 14 fig. 1, pl. 18 figs 3, 5.
1972 *Gobichara tenera* Karczewska & Ziembińska-Tworzydło, pp. 78–79, fig. 14, pl. 17 figs 1–6.
1972 *Gobichara alba* Karczewska & Ziembińska-Tworzydło, pl. 18 figs 1–2.

Material. The sample obtained at depth of 307.85 m contained about 70 gyrogonites each. Approximately 200 gyrogonites in total were obtained from a further 13 samples from other depths in the borehole studied (Fig. 4).

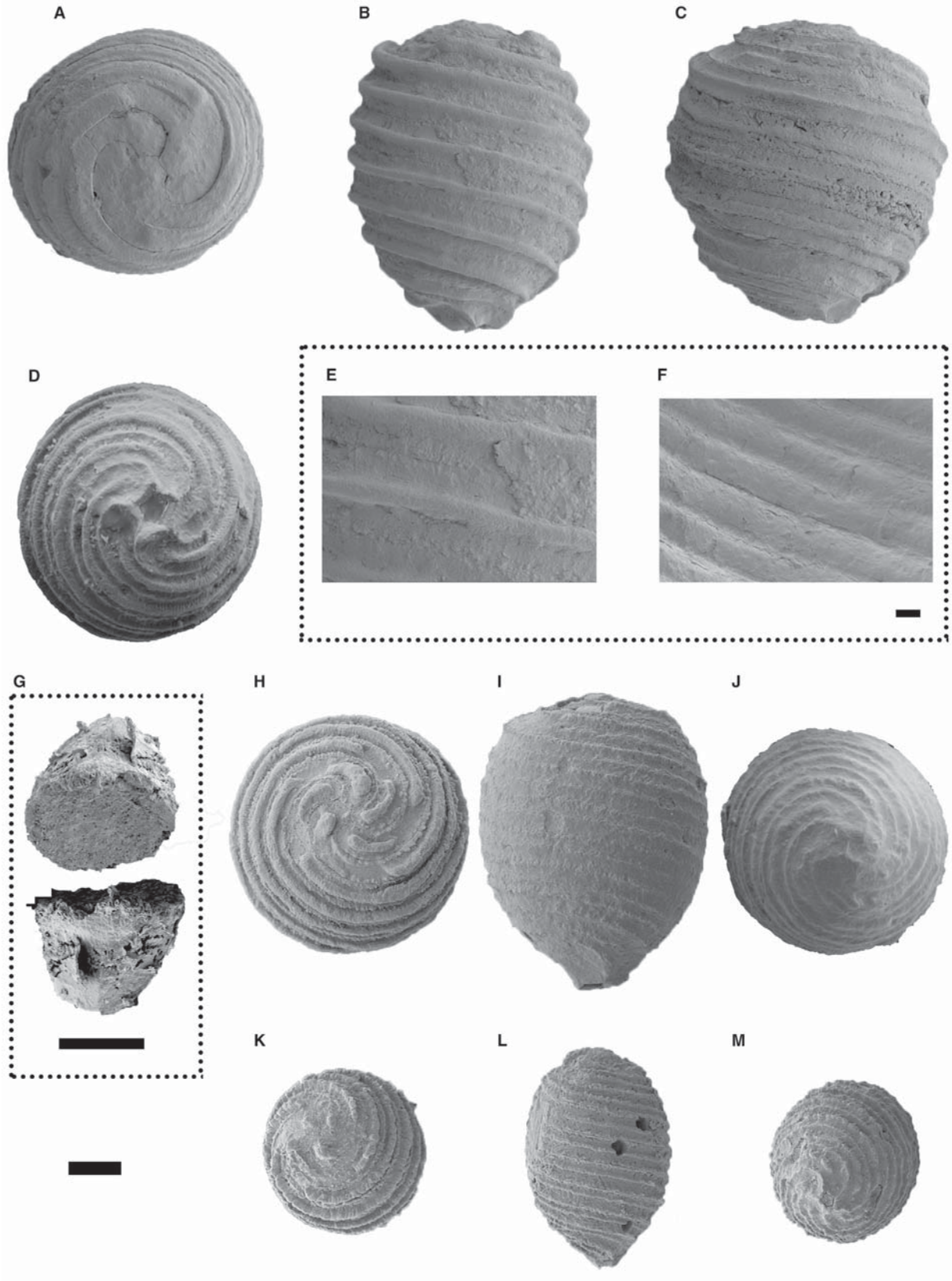
A
B
C
D
E
F
G
H
I
J
K
L
M

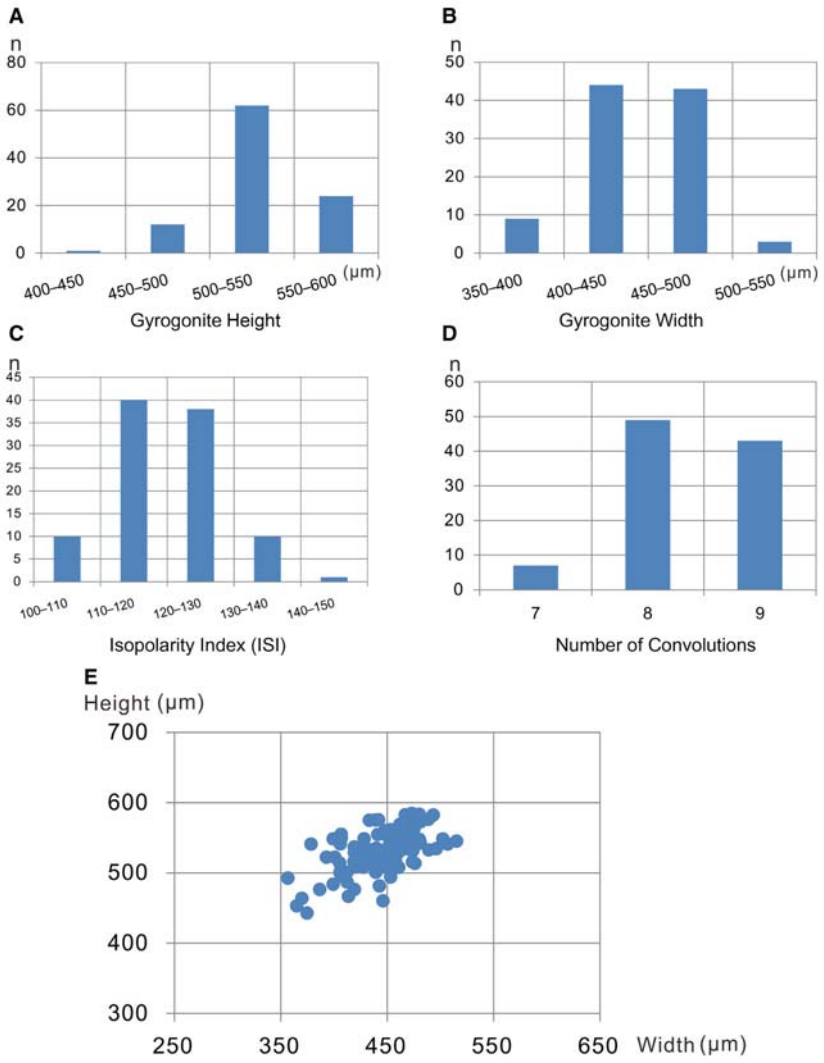

FIG. 9. Biometric data of *Microchara gobica* (99 gyrogonites from the depth of 809.77 m) in the SK-1 (North) borehole, Songliao Basin. A, height. B, width. C, isopolarity index (ISI). D, number of convolutions. E, dispersion graph of height/width. Colour online.

Description. Gyrogonites are small to medium in size, 358–467 μm high (mean: 413 μm) and 245–369 μm wide (mean: 307 μm). Isopolarity index ranges from 107 to 161, prolate spheroidal and subprolate in shape; 8–10 (mostly 8–9) convolutions are visible in lateral view. Spiral cells are 40–50 μm wide, concave, ornamented with continuous, sometimes wavy mid-cellular crests, with the same width as and parallel to the sutures. The mid-cellular crest disappears around the apex periphery, to form generally prominent comma-shaped nodules in the apical centre. In contrast, the mid-cellular crest is continuous to the base, reaching the basal pore. Apex is rounded. Base pointed, sometimes elongated in a short column, ending with a pentagonal basal pore, 20–30 μm in diameter. Basal plate is undivided, thin, and pentagonal, not visible from the exterior.

Remarks. Genera *Microchara* and *Gobichara* were synonymized by Feist *et al.* (2005). *Gobichara deserta* in particular was synonymized with *Microchara cristata* based on material from the Pingyi Basin by Li *et al.* (2016). Karczewska & Ziembińska-Tworzydło (1972) established the new genus *Gobichara*, and included five new species within it, that is, *G. deserta*, *G. nigra*, *G. rubra*, *G. tenera* and *G. alba*. The same authors reported that the differences between these species mainly concerned the general

FIG. 8. Charophytes from the Songliao Basin. A–G, *Microchara gobica*: A, apical view, PB22624; B–C, lateral view, PB22625, PB22626; D, basal view, PB22627; E–F, details of sutures and intercellular crests; F, PB22628; G, basal plate, PB22629; sample depth: A–F, 813.57 m; G, 799.93 m. H–M, *Microchara cristata*: H, K, apical view, PB22630, PB22631; I, L, lateral view, PB22632, PB22633; J, M, basal view, PB22634, PB22635; sample depth: H–J, 442.5 m; K–L, 299.74 m; M, 339.95 m. Scale bars represent: 100 μm (lower left, A–D, H–M); 20 μm (E, F); 50 μm (G).

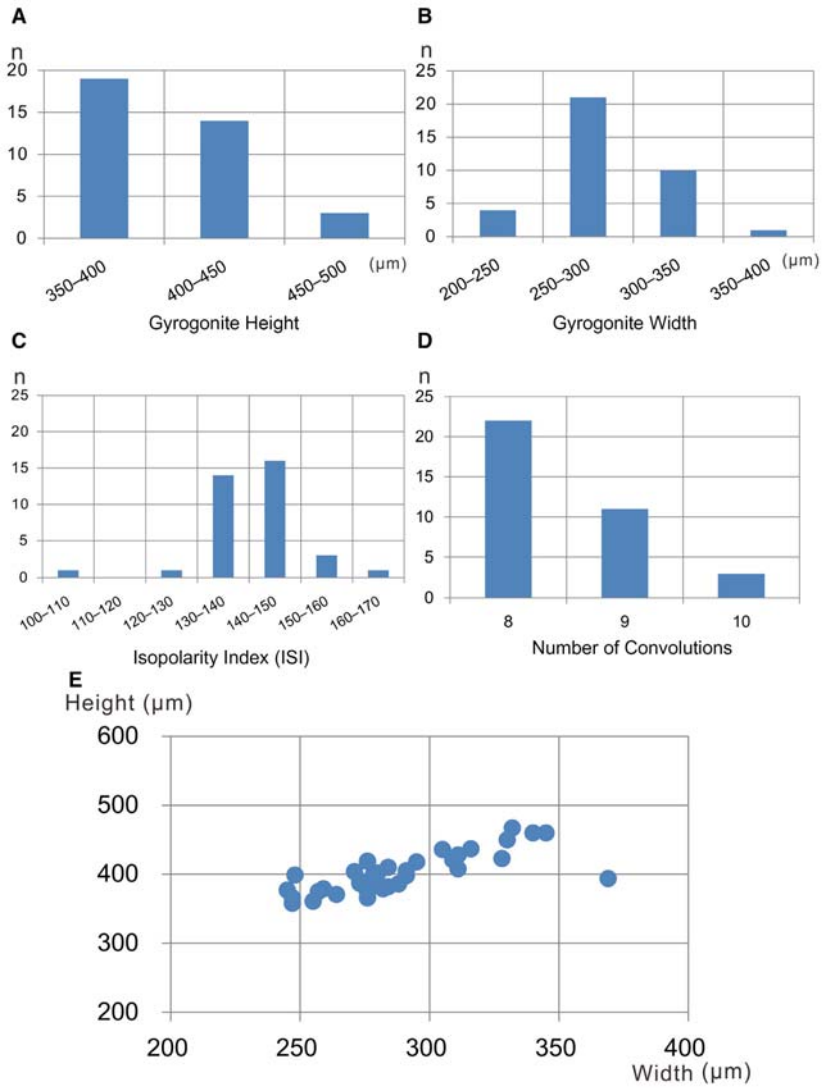

FIG. 10. Biometric data of *Microchara cristata* (36 gyrogonites from the depth of 307.85 m) in the SK-1 (North) borehole, Songliao Basin. A, height. B, width. C, isopolarity index (ISI). D, number of convolutions. E, dispersion graph of height/width. Colour online.

morphology of gyrogonites, traces of a mid-cellular crest, shape of apical nodules, and equatorial angle of spiral cells. In the present study, intermediate specimens between the five species were found within large populations, showing that they probably represent the variation range of one species. Therefore, they are all considered to be younger synonyms of *Microchara cristata*. As already noted by Grambast (1971), *M. cristata* is a species with relatively high intraspecific polymorphism in the gyrogonite shape.

Distribution. Microchara cristata was distributed throughout Eurasia. It was first reported in the Campanian (lower Rognacian local stage) in Rognac (Provence, France) by Grambast (1971). It was subsequently found in several Campanian and Maastrichtian localities of France (Feist & Freytet 1983; Lepicard *et al.* 1985; Massieux *et al.* 1985), Spain (Feist & Colombo 1983; Masriera & Ullastre 1988; Galbrun *et al.* 1993; Villalba-Breva *et al.* 2012; Villalba-Breva & Martín-Closas 2013), Rumania (Villalba-Breva & Martín-Closas 2013), and in the Maaastrichtian

FIG. 11. Charophytes from the Songliao Basin. A–D, *Microchara leiocarpa*: A, apical view, PB22636; B, lateral view, PB22637; C, basal view, PB22638; D, basal plate, PB22639; sample depth, 855.61 m. E–H, *Microchara prolixa*: E, apical view, PB22640; F, lateral view, PB22641; G, basal view, PB22642; H, basal plate, PB22643; sample depth, 306.7 m. I–K, *Chara changzhouensis*: I, apical view, with the arrow indicating the sinous intercellular crest, PB22644; J, lateral view, PB22645; K, basal view, PB22646; sample depth, 306.7 m. L–O, *Nemegtichara prima*: L, apical view, PB22647; M, lateral view, PB22648; N, basal view, PB22649; O, basal plate, PB22650; sample depth: L–N, 403.5 m; O, 415.53 m. Scale bars represent: 100 μm (lower right, A–C, E–G, L–O; middle right, I–K); 20 μm (D, H).

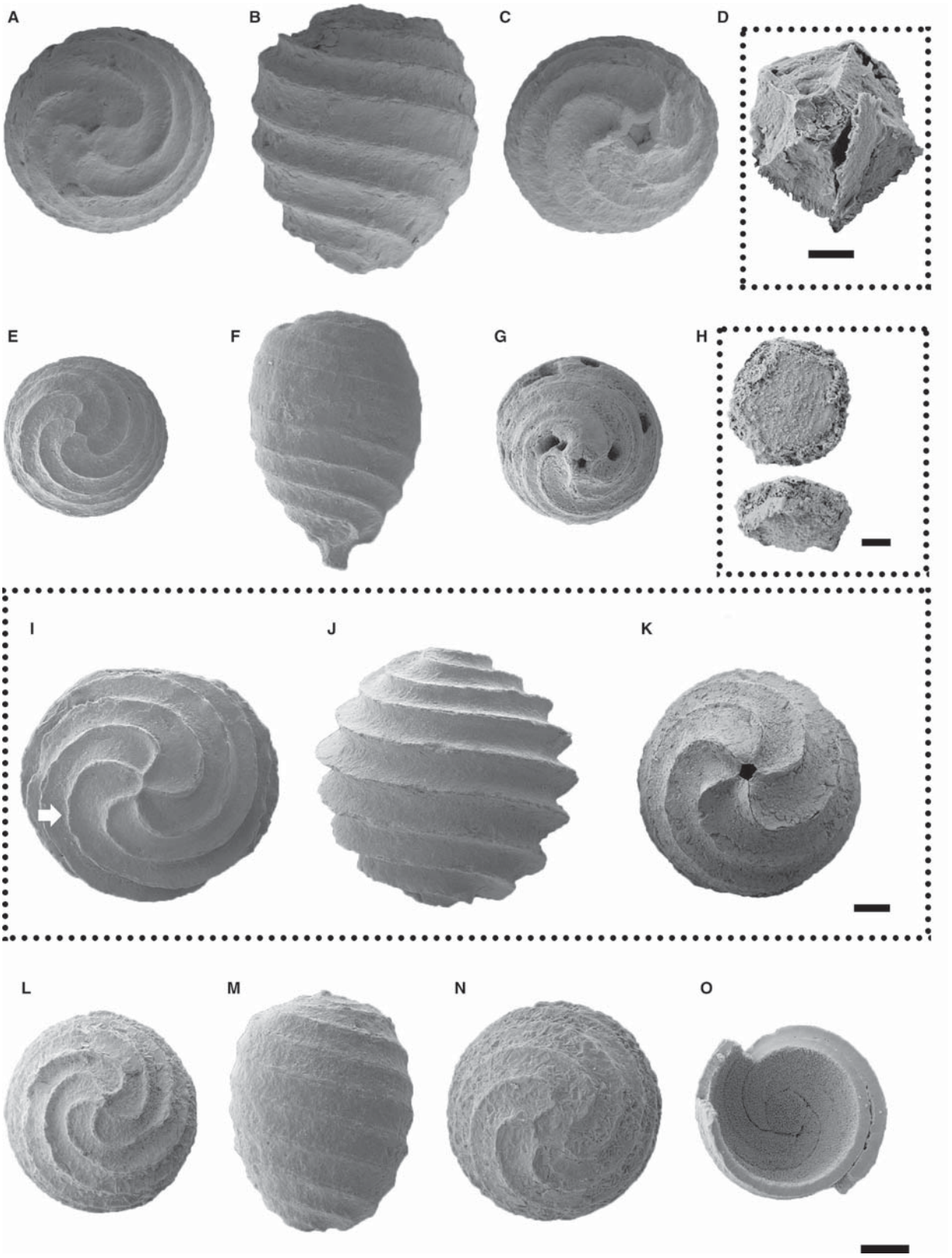
A
B
C
D
E
F
G
H
I
J
K
L
M
N
O

of Mongolia (Karczewska & Ziembińska-Tworzydło 1972). In the Campanian to Maastrichtian of China, it shows a wide distribution in the Songliao Basin (Wang *et al.* 1985; Li *et al.* 2013), Shalamulun area (Liu 1987), Junggar Basin (Yang *et al.* 2005, 2008), Pingyi Basin (Li *et al.* 2016), North Jiangsu Basin (Wang *et al.* 1982), Jianghan Basin (Li 1998; Li *et al.* 2010), Hunan Province (Hu & Zeng 1982), and Nanxiong Basin (Huang 1988).

Microchara leiocarpa Grambast, 1971
Figures 11A–D, 12

1971 *Microchara leiocarpa* Grambast, pp. 33–35, figs 20, 21, pl. 26 figs 1–6, pl. 27 figs 1–8.
1985 *Hornichara anguangensis* Wang *et al.*, pp. 51–52, pl. 20 figs 6–7.

Material. About 30 gyrogonites occurred in from each of the samples obtained at depths of 813.57 and 809.77 m. Smaller populations occur in 16 samples from other depths in the borehole studied (Fig. 4).

Description. Gyrogonites medium in size, 453–605 μm high (mean: 529 μm) and 392–546 μm wide (mean: 469 μm). Isopolarity index ranges from 101 to 135, ovoidal in shape; 7–9 convolutions are visible in lateral view. Spiral cells are concave, 80–100 μm wide in size, usually devoid of ornamentation. The sutures are prominent, bicarinate in most samples. Apex is flat to rounded, without any periapical or apical modification. Base is rounded to tapering, displaying a pentagonal funnel. Basal pore is 40–60 μm in size. Basal plate is in the shape of a pentagonal pyramid (Fig. 11D).

Remarks. Microchara leiocarpa is characterized by its psilocharoid apex and ovoidal shape. It may be compared with other unornamented species of the genus *Microchara*, such as *M. laevigata* Grambast & Gutiérrez, 1977 and *M. tunicata* Grambast & Gutiérrez, 1977. With regard to size, *M. tunicata* is the largest, being on average 575–650 μm in height and 475–550 μm in width, followed by *M. leiocarpa* at 527–575 μm in height and 450–500 μm in width, while the smallest is *M. laevigata*, which is 300–400 μm in height and 300–400 μm in width. As regarding general shape, *M. leiocarpa* is rounded ovoidal with a tapering base. *M. laevigata* is prolate spheroidal with a round base and

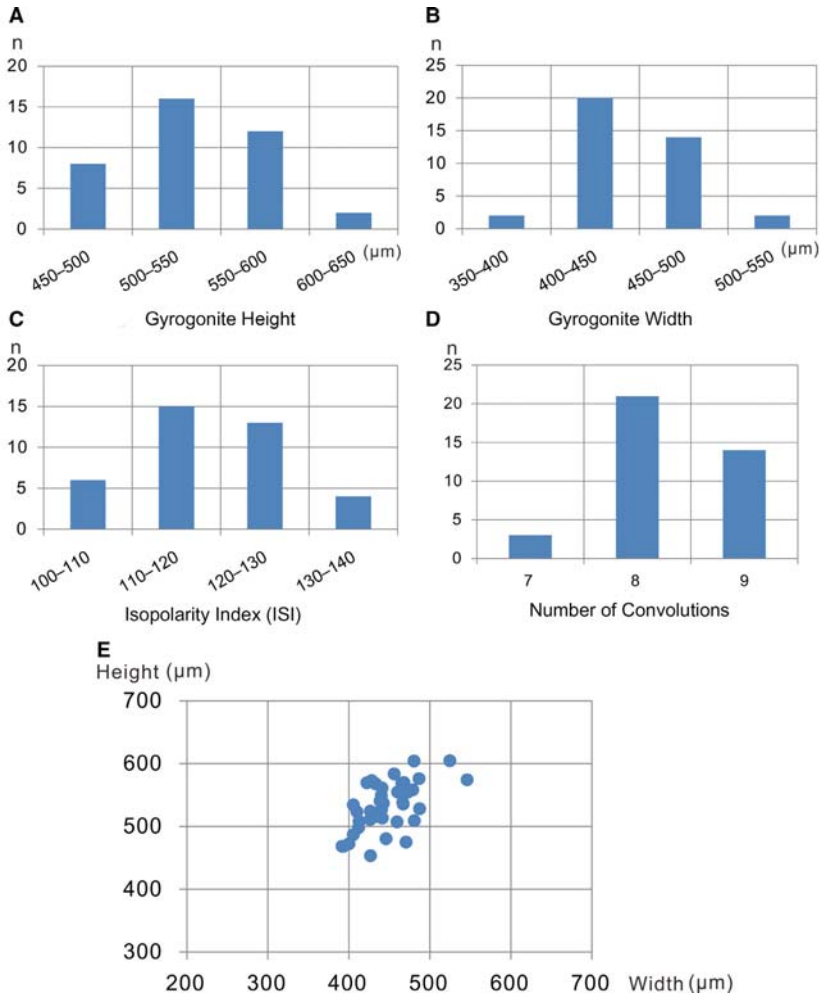

FIG. 12. Biometric data of *Microchara leiocarpa* (38 gyrogonites from the depth of 813.57 m) in the SK-1 (North) borehole, Songliao Basin. A, height. B, width. C, isopolarity index (ISI). D, number of convolutions. E, dispersion graph of height/width. Colour online.

never displays a tapering base. *M. tunicata* is prolate with a tapering base. With respect to ornamentation, apical nodules are sometimes developed in *M. leiocarpa*, but never in *M. laevigata* or *M. tunicata*. The number of lateral convolutions is similar in the three species.

Distribution. Microchara leiocarpa was first reported in the Campanian (lower Rognacian local stage) of Rognac (Provence, France) by Grambast (1971).

Microchara prolixa (Wang *et al.*, 1985) comb. nov.
Figures 11E–H, 13

1985 *Hornichara prolixa* Wang *et al.*, pp. 50–51, pl. 19 fig. 8; pl. 20 figs 1–5.

Material. More than 100 gyrogonites occurred in a sample taken at the depth of 403.5 m. Smaller populations yielded a total of 300 gyrogonites obtained from 21 samples at other depths in the borehole studied (Fig. 4).

Description. Gyrogonites medium in size, 407–574 μm high (mean 491 μm) and 279–393 μm wide (mean 336 μm), Isopolarity index ranges from 120 to 170, prolate ovoidal in shape; 8–10 convolutions are visible in lateral view. Spiral cells are concave, 49–71 μm wide, devoid of ornamentation. Apex is round, sometimes slightly prominent, without spiral cell modifications. Base is tapering, with a well-developed basal column. Basal pore is pentagonal, 10–20 μm in diameter, forming a small funnel. Basal plate is undivided, thin, and pentagonal.

Remarks. The shape and basal plate of *M. prolixa* is characteristic of the genus *Microchara*. The apex is not as prominent as in *Hornichara*, hence the new combination appears well-justified.

Distribution. This species has been reported in the second member of the Mingshui Formation belonging to the

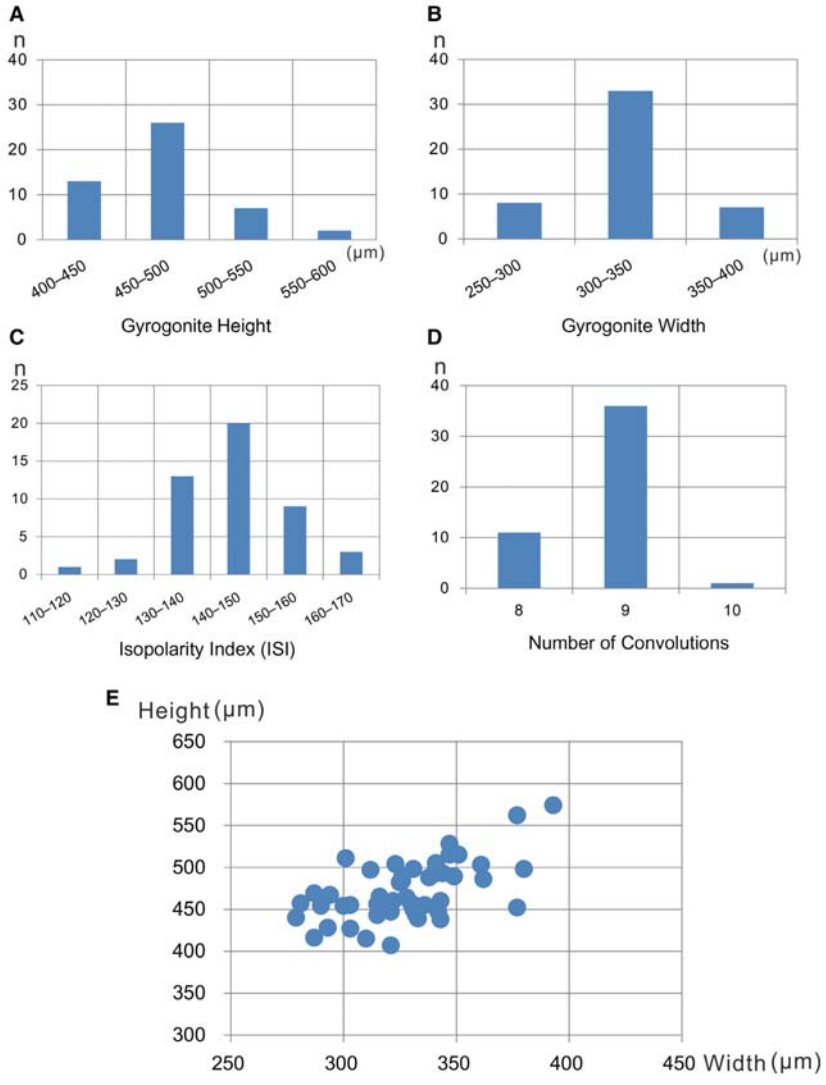

FIG. 13. Biometric data of *Microchara prolixa* (48 gyrogonites from the depth of 331.42 m) in the SK-1 (North) borehole, Songliao Basin. A, height. B, width. C, isopolarity index (ISI). D, number of convolutions. E, dispersion graph of height/width. Colour online.

Maastrichtian and early Paleocene (Wang *et al.* 1985) and in the Late Cretaceous to early Paleocene Ziniquanzi Formation in the Junggar Basin, Xinjiang Uygur Autonomous Region (Yang *et al.* 2005).

Genus CHARA Vaillant, 1719
Chara changzhouensis (Huang & S. Wang *in* Z. Wang, 1978*b*) comb. nov.
Figure 11I–K

1978*b* *Grovesichara changzhouensis* Huang & S. Wang *in* Z. Wang, p. 112, pl. 3 figs 1–18.

Material. 35 gyrogonites were obtained from a sample at the depth of 317.03 m. Smaller populations occurred in eight samples from other depths in the borehole studied (Fig. 4).

Description. Gyrogonites are medium to large in size, 720–798 μm high (mean: 759 μm) and 613–739 μm wide (mean: 676 μm). Isopolarity index ranges from 106 to 127 (mean: 117), generally sphaeroidal to subprolate in shape; 8–9 convolutions are visible in lateral view. Spiral cells are concave, occasionally convex, 120–130 μm wide, with high intercellular crests, sometimes wavy (Fig. 11I). Apex is rounded, without periapical modifications but with slightly enlarged spiral cell endings. Base is round, with a pentagonal basal pore, 50–60 μm in diameter. Basal plate is undivided and in the shape of a pentagonal pyramid, not visible from the exterior.

Remarks. The main features of *Chara changzhouensis* gyrogonites are a globular shape, wide spiral cells, and prominent sutures. This species cannot be accommodated within the genus *Grovesichara* as proposed by earlier authors since it does not display any periapical modification, and also because the basal plate is not visible from the exterior. Hence, a new combination within the genus *Chara* is proposed based mainly in the little modifications of spiral cells in the apex.

Distribution. Chara changzhouensis was first reported in the Fangjiahe, Zhaizishan and Yangqi formations (upper Paleocene? – lower Eocene deposits) in the Jianghan Basin (Wang 1978*b*). Later, it was also found in the Mingshui Formation (Upper Cretaceous – Paleocene deposits) in the Songliao Basin (Wang *et al.* 1985), the Erliandabusu Formation (Upper Cretaceous – Paleocene deposits) in Inner Mongolia (Liu 1987), the Ziniquanzi Formation (Upper Cretaceous – Paleocene deposits) in the Junggar Basin (Yang *et al.* 2005), in the Taizhou Formation, Funing Group, and Dainan Formation (Upper Cretaceous? – Paleogene deposits) in the North Jiangsu Basin (Wang *et al.* 1982) and in the Nanxiong and Shanghu formations (Upper Cretaceous – Paleocene deposits) in the Nanxiong Basin (Huang 1988). It is important to note that the age of these formations is only approximate and has not been established by other means.

Genus NEMEGTICHARA Karczewska & Ziembińska-Tworzydło, 1972
Nemegtichara prima Karczewska & Ziembińska-Tworzydło, 1972
Figure 11L–O

1972 *Nemegtichara prima* Karczewska & Ziembińska-Tworzydło, pl. 7 figs 1, 3–4; pl. 8 figs 1–2, 5–6; pl. 9, fig. 2; pl. 24 figs 1, 3–4; text-figs 2–3.

Material. 43 gyrogonites were collected from a sample taken at the depth of 442.5 m. Smaller populations occurred in 10 samples from other depths in the borehole studied (Fig. 4).

Description. Gyrogonites are medium in size, 415–498 μm high (mean: 457 μm) and 347–514 μm wide (mean: 431 μm). Isopolarity index ranges from 116 to 128, resulting in a cylindrical shape; 7–9 convolutions are visible in lateral view. Spiral cells, 70–90 μm wide, are concave and separated by sutures that are sometimes bicarinate. Apex is slightly conical with a pointed apical centre and the periapical area shows a moderate thinning of spiral cells. Base is round to flat, with a pentagonal basal pore, 60–70 μm in diameter. Basal plate is large, undivided, and pentagonal, visible from the exterior.

Remarks. The genus *Nemegtichara* is characterized by moderate thinning of spiral cells in the apical zone and a pentagonal basal plate that is visible from the exterior. It differs from the genus *Lamprothamnium* mainly because the apex of *Nemegtichara* is slightly conical with moderate thinning of spiral cells, whereas that of *Lamprothamnium* is truncated and displays a deep periapical depression. In addition, the basal plate of the latter is not visible from the exterior.

Distribution. This species was first reported in the White beds (Palaeogene deposits) of the Nemegt Basin, Gobi

FIG. 14. Charophytes from the Songliao Basin. A–C, *Lamprothamnium ellipticum*: A, apical view, PB22651; B, lateral view, PB22652; C, basal view, PB22653; sample depth, 855.61 m. D–F, *Nodosochara* (*Turbochara*) *specialis*: D, apical view, PB22654; E, lateral view, PB22655; F, basal view, PB22656; sample depth, 379.73 m. G–I, *Lychnothamnus yuntaishanensis*: G, apical view, PB22657; H, lateral view, PB22658; I, basal view, PB22659; sample depth, 968.48 m. J–O, *Lychnothamnus* aff. *vectensis*: J, M, apical view, PB22660, PB22661; K, N, lateral view, PB22662, PB22663; L, O, basal view, PB22664, PB22665; sample depth, 317.03 m. Scale bars represent 100 μm.

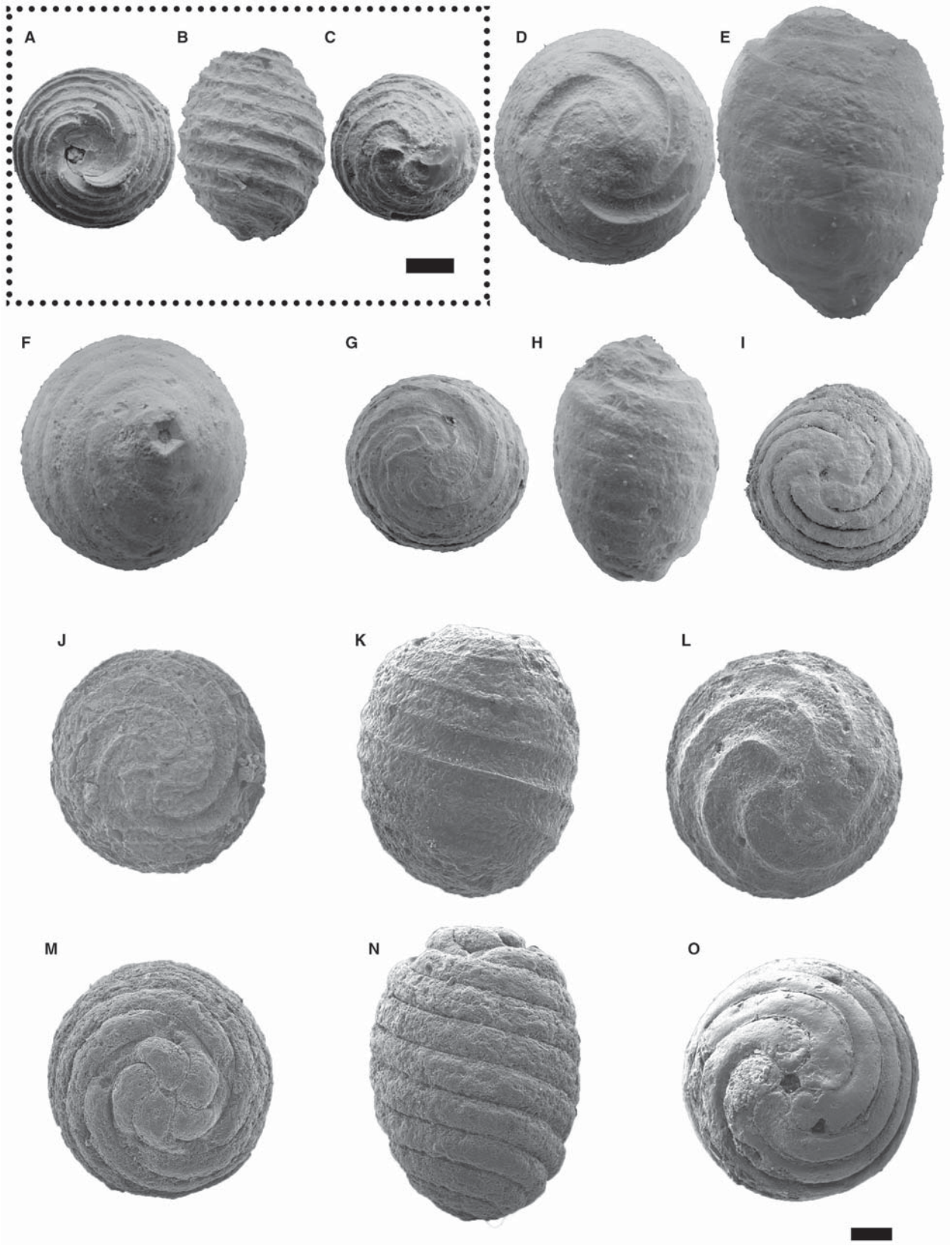
A
B
C
D
E
F
G
H
I
J
K
L
M
N
O

Desert, Mongolia (Karczewska & Ziembińska-Tworzydło 1972). Later, it was also found in the Mingshui Formation of the Songliao Basin, north-east China (Wang *et al.* 1985; Li *et al.* 2013).

Genus LAMPROTHAMNIUM Groves, 1916
Lamprothamnium ellipticum (Wang *et al.*, 1985) Li & Martín-Closas *in* Li *et al.*, 2016
Figure 14A–C

1976 *Euaclistochara mundula* comb. nov.; Wang *et al.*, pp. 71–72.
1985 *Euaclistochara mundula* var. *elliptica* var. nov.; Wang *et al.*, p. 25, pl. 4 figs 4–8.
2016 *Lamprothamnium ellipticum* comb. nov.; Li & Martín-Closas *in* Li *et al.*, fig. 4E–G.

Material. 10 gyrogonites were obtained from one sample at a depth of 809.77 m. Smaller populations occurred in 11 samples at other depths in the borehole studied (see Fig. 4).

Description. Small gyrogonites, 335–386 μm high (mean: 361 μm) and 256–335 μm wide (mean: 296 μm). Isopolarity index ranges from 108 to 141, generally prolate in shape. Spiral cells are concave to planar, 40–60 μm wide, devoid of ornamentation, with 10–11 convolutions in lateral view. The apex is truncated and displays a deep apical depression that could appear to be a wide pore if not completely clean of sediment. The spiral cells bend sharply down into the depression and then shortly emerge again at the bottom of it to join in the centre. The base is rounded, with a small and circular basal pore, 20–30 μm in size. Basal plate is prismatic and unicellular (Wang *et al.* 1985; Li *et al.* 2016).

Remarks. The size of the gyrogonites of this species in the Pingyi and Songliao basins are within the same range. However, the material from the Pingyi Basin is heavily encrusted, thus the edge of the apical depression shows an exceedingly thick rim. The material from this study provides new information about the shape of the periapical area, clearly showing that the thick apical rim observed in Pingyi was due to external encrustation and that the spiral cells bend deeply downward within the apical depression in a similar way as in some extant *Lamprothamnium*.

Wang *et al.* (1985) found the species described here in the Upper Cretaceous of the Songliao Basin and placed it within *E. mundula*. However, the assemblage of characters, a unicellular basal plate, together with a very deep apical depression similar to a crater and bearing a closed apex at the bottom, makes *Euaclistochara* very similar to extant gyrogonites of *Lamprothamnium succintum* as studied and illustrated by Soulie-Märsche (1989). In consequence, Li *et al.* (2016) proposed placing this type of gyrogonite within the genus *Lamprothamnium*. This new combination was proposed to include all charophyte fructifications attributed to *Euaclistochara mundula* by previous authors. However, the type material of this species defined in North America by Peck (1941, 1957) is provisionally not included since its apex and basal plate are still poorly known.

Distribution. Lamprothamnium ellipticum was found in the Upper Cretaceous Sifangtai and Mingshui formations in the Songliao Basin, north-east China, by Wang *et al.* (1985) and in the Upper Cretaceous Gucheng Formation, Pingyi Basin, Shandong Province (Li *et al.* 2016) in China.

Genus NODOSOCHARA Mädler, 1955
Subgenus TURBOCHARA (Wang, 1978*a*) comb. nov.
Nodosochara (*Turbochara*) *specialis* (Wang, 1978*a*) comb. nov.
Figure 14D–F

1978*a* *Turbochara specialis* Wang, p. 78, pl. 6 figs 1–9.

Material. 15 gyrogonites were obtained from a sample taken at the depth of 465.23 m. Smaller populations occurred in 10 samples from other depths in the borehole studied (Fig. 4).

Description. Gyrogonites are medium to large, 612–737 μm high (mean: 675 μm) and 474–556 μm wide (mean: 515 μm). Isopolarity index ranges from 125 to 139, subprolate and prolate ovoid in shape; 8–10 convolutions are visible in lateral view. Spiral cells are planar to convex, 80–95 μm wide, devoid of ornamentation. Apex is flat, with periapical thinning and different ranges of narrowing, forming a conical apical centre. Base is tapering, ending in a short projection with a small funnel and a small pentagonal pore, 30 μm in diameter. Basal plate not observed.

Remarks. Turbochara is treated here as a subgenus of *Nodosochara.* Feist *et al.* (2005) proposed its synonymy with *Nodosochara* based on the narrowing and thinning of the spiral cells in the periapical zone, in combination with a small basal pore. However, the regularly slight apical narrowing of spiral cells in *Turbochara* gyrogonites represents a clear variation in comparison with the strong narrowing of these cells in the type *Nodosochara*.

Distribution. Nodosochara (*Turbochara*) *specialis* has been reported in the Upper Cretaceous of the Paomagang Formation in the Jianghan Basin (Wang 1978*a*) and in the Sifangtai Formation and the second member of the Mingshui Formation in the Songliao Basin (Wang *et al.* 1985; Li *et al.* 2013).

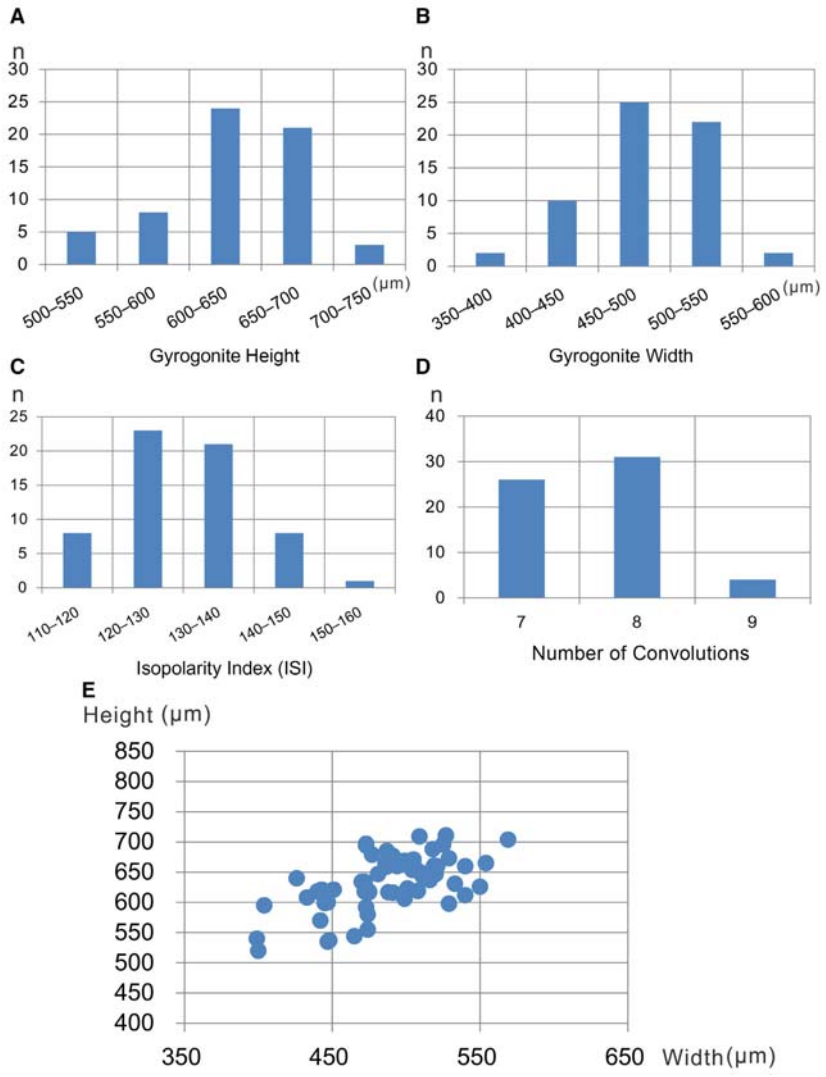

FIG. 15. Biometric data of *Lychnothamnus* aff. *vectensis* (61 gyrogonites from the depth of 331.42 m) in the SK-1(North) borehole, Songliao Basin. A, height. B, width. C, isopolarity index (ISI). D, number of convolutions. E, dispersion graph of height/width. Colour online.

Genus LYCHNOTHAMNUS (Ruprecht, 1845) von Leonhardi, 1863 emend. Braun *in* Braun & Nordstedt, 1882

Lychnothamnus yuntaishanensis (Wang, 1978a) comb. nov.

Figure 14G–I

1978*a* *Grambastichara yuntaishanensis* Wang, p. 78, pl. 7 figs 21–32.

Material. 35 gyrogonites were obtained from a sample at the depth of 809.77 m. Smaller populations occurred in eight samples at other depths in the borehole studied (Fig. 4).

Description. Gyrogonites are medium in size, 500–658 μm high (mean: 579 μm) and 392–534 μm wide (mean: 463 μm). Isopolarity index ranges from 107 to 142, the gyrogonite being ovoidal in shape; 8–10 convolutions are visible in lateral view. Spiral cells are convex, 60–70 μm in height, usually devoid of ornamentation, occasionally bearing small prominent nodules distributed unevenly. Sutures are simple, not bicarinate. Apex is flat, with a periapical furrow showing apical thinning but not narrowing of spiral cells, which results in a prominent apical centre. The base is first tapering, later becoming truncated. It displays a pentagonal basal pore, 30–50 μm in diameter.

Remarks. The main diagnostic character of the subgenus is the apical thinning of the spiral cells without narrowing. This species was first included within the genus *Grambastichara* (now a synonym for *Chara*) by Wang *et al.* (1985) because of the narrowing of spiral cells in the periapical region. However, from the pictures provided by these authors, the cells in the apical centre become slightly larger, without any previous narrowing. Therefore, a new combination within the genus *Lychnothamnus* is proposed here.

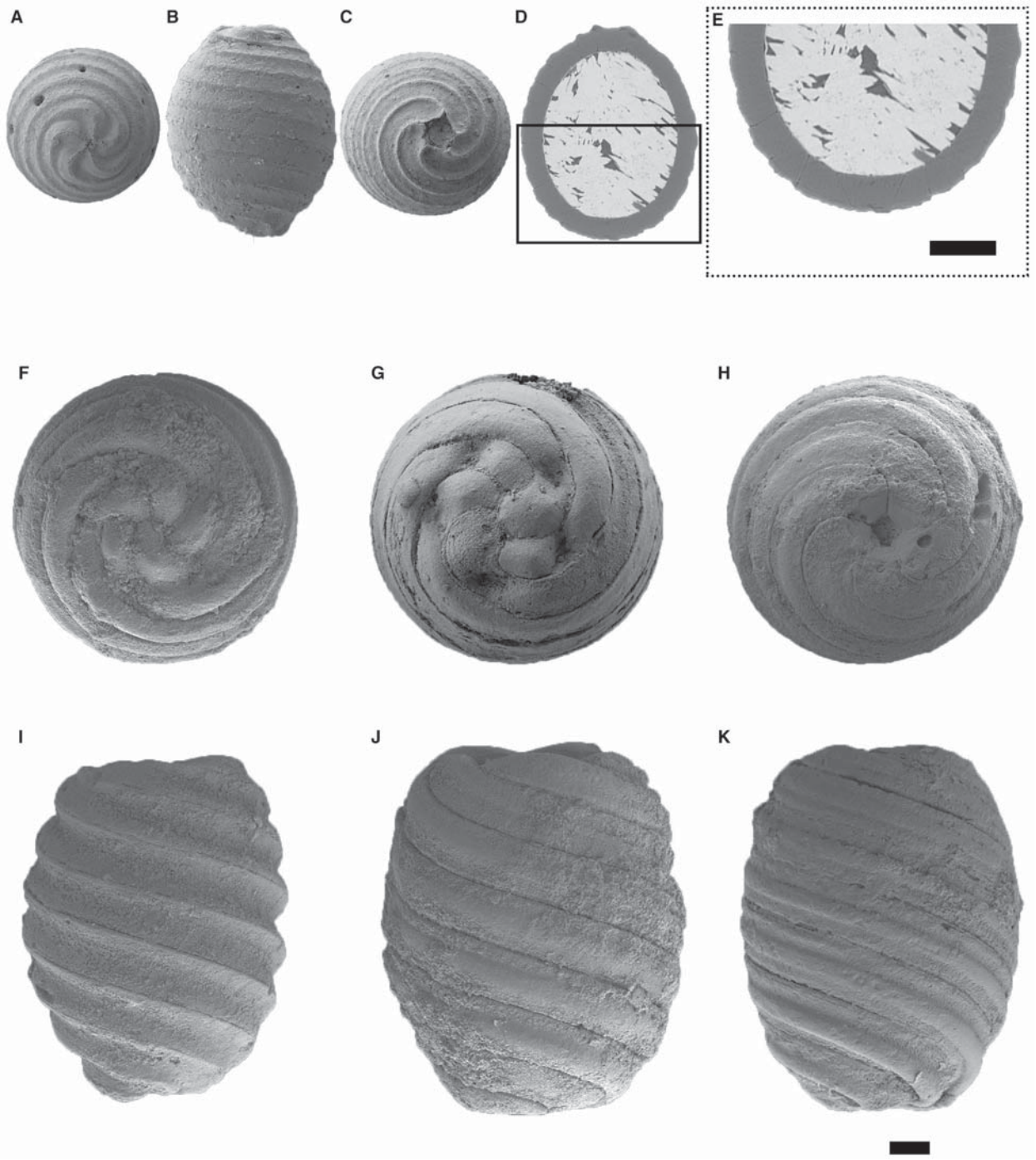

FIG. 16. Charophytes from the Songliao Basin. A–E, *Collichara taizhouensis*: A, apical view, PB22666; B, lateral view, PB22667; C, basal view, PB22668; D–E, μCT image of section and basal plate, PB22669; sample depth, 317.03 m. F–K, *Peckichara sinuolata*: F–G, apical view, PB22670, PB222671; H, basal view, PB22672; I–K, lateral view, PB22673–PB22675; sample depth, 325.59 m. Scale bars represent: 100 μm (lower right, A–D, F–K; upper right, E).

Distribution. Lychnothamnus yuntaishanensis has been reported from the Upper Cretaceous to Paleocene? deposits in the Yuntaishan Formation in the Jianghan Basin (Wang 1978*a*) and in the Sifangtai Formation in the Songliao Basin (Wang *et al.* 1985).

Lychnothamnus aff. *vectensis* (Groves, 1926) Soulié-Märsche, 1989
Figures 14J–O, 15

1926 *Chara vectensis* Groves, p. 172, pl. 2 figs 2–8.
1958 *Stephanochara vectensis* comb. nov.; Grambast, p. 158.
1989 *Lychnothamnus vectensis* comb. nov.; Soulié-Märsche, p. 160.

Material. More than 100 gyrogonites were obtained from each sample at the depths of 325.59 and 317.03 m. Smaller populations occurred in nine samples at other depths in the borehole studied (Fig. 4).

Description. Gyrogonites are medium to large in size, 520–711 μm high (mean: 616 μm) and 399–569 μm wide (mean: 484 μm). Isopolarity index ranges from 113 to 150 (mean 132), being ellipsoidal in shape; 7–9 convolutions are visible in lateral view. Spiral cells are 80–100 μm wide, planar to convex, separated by simple sutures. Apex is round, with well-marked periapical thinning, without nodules on concave specimens, whereas in convex specimens there is a well-developed, apical rosette with prominent nodules with height ranging from 0 to 102.9 μm, joining completely at the apical centre to form a highly protruding and compact cap. Base is round, with a pentagonal basal pore, 50 μm in diameter, sometimes forming a small pentagonal funnel.

Remarks. The specimens studied are similar to *Lychnothamnus vectensis* from the Ebro Basin (Sanjuan & Martín-Closas 2015) as regards size, shape, number of convolutions, ISI, width of spiral cells, and some features of the apex and the base. However, it differs from the type *L. vectensis* from the Isle of Wight (Groves 1926; Sanjuan & Martín-Closas 2015) in the general presence of apical nodules throughout the population and the more prominent apical rosette, with nodules fused instead of being separated. Furthermore, the ages of the two species are very different, since in Europe, *Lychnothamnus vectensis* is latest Priabonian to early Rupelian in age. Further studies are required to clarify the relationship between the Chinese *L.* aff *vectensis* and the late Eocene – early Oligocene European species.

Genus COLLICHARA S. Wang & Zhang *in* Wang *et al.*, 1982
Collichara taizhouensis S. Wang & Zhang *in* Wang *et al.*, 1982
Figures 16A–E, 17

1982 *Collichara taizhouensis* S. Wang & Zhang *in* Wang *et al.*, p. 49, pl. 26 figs 1–8.

Material. Four populations represented by only a few specimens each yielded a total of about 50 gyrogonites from samples at the depths of 317.03, 307.85, 307.05, and 306.7 m in the borehole studied (Fig. 4).

Description. Gyrogonites are medium in size, 479–582 μm high (mean: 531 μm) and 375–467 μm wide (mean: 421 μm). Gyrogonites are ellipsoidal in shape with an isopolarity index ranging from 116 to 138; 9–12 convolutions are visible in lateral view. Spiral cells concave to planar, 40–60 μm wide, without ornamentation. The apex is truncated, sometimes showing some widening of the spiral cells at the apex centre. Cells in the periapical area show an increased thickening of the calcification at both sides of the cell suture, rendering the mid-cellular area deeply depressed (Fig. 16A). Base is rounded with a large pentagonal pore, 40–60 μm in diameter. The basal plate is unicellular, large, and visible from the exterior, in the shape of a truncated pentagonal pyramid, sometimes with rounded edges, its height being about half the maximum width (Fig. 16D, E).

Remarks. The main diagnostic feature of *Collichara taizhouensis* is the unique calcification of the cell margins in the periapical area. The genus *Collichara* was named by S. Wang & Zhang *in* Wang *et al.* (1982) after the Latin word *collis*, meaning neck, because of the shape of the apical area in lateral view, showing a short inflection, similar to a neck, before the apical truncation. It is similar to the genus *Sphaerochara* in displaying a large basal plate visible from the exterior of the gyrogonite. However, the shape of the basal plate in *Sphaerochara* differs in being as thick as it is wide, with upper and lower faces pentagonal to stellate. Furthermore, the apical features are also distinct from *Sphaerochara* since this genus displays a rounded apex and lacks any periapical modification.

Distribution. Collichara taizhouensis was first reported in the Taizhou Formation and at the base of the Funing Group (uppermost Cretaceous? – lower Paleocene deposits) in the North Jiangsu Basin (Wang 2004; Wang *et al.* 1982). Later, it was also reported in the second member of the Mingshui Formation in the Songliao Basin (Wang *et al.* 1985).

Genus PECKICHARA Grambast, 1957
Peckichara sinuolata (Z. Wang & Lin *in* Wang *et al.* 1982) comb. nov.
Figures 16F–L, 18

1978 nomen nudum *Neochara sinuolata*; Wang & Lin *in* Wang *et al.*, p. 41, pl. 17 fig. 5.
1982 *Neochara sinuolata* Z. Wang & Lin *in* Wang *et al.*, p. 43, pl. 24 figs 1–7.

Material. More than 100 gyrogonites were obtained from a sample taken at the depth of 325.59 m. Smaller populations occurred at the depth of 329.06 m in the borehole studied (Fig. 4).

Description. Gyrogonites are large in size, 789–1060 μm high (mean: 925 μm) and 569–805 μm wide (mean: 687 μm). They are barrel-shaped, subprolate, occasionally prolate in shape, with an

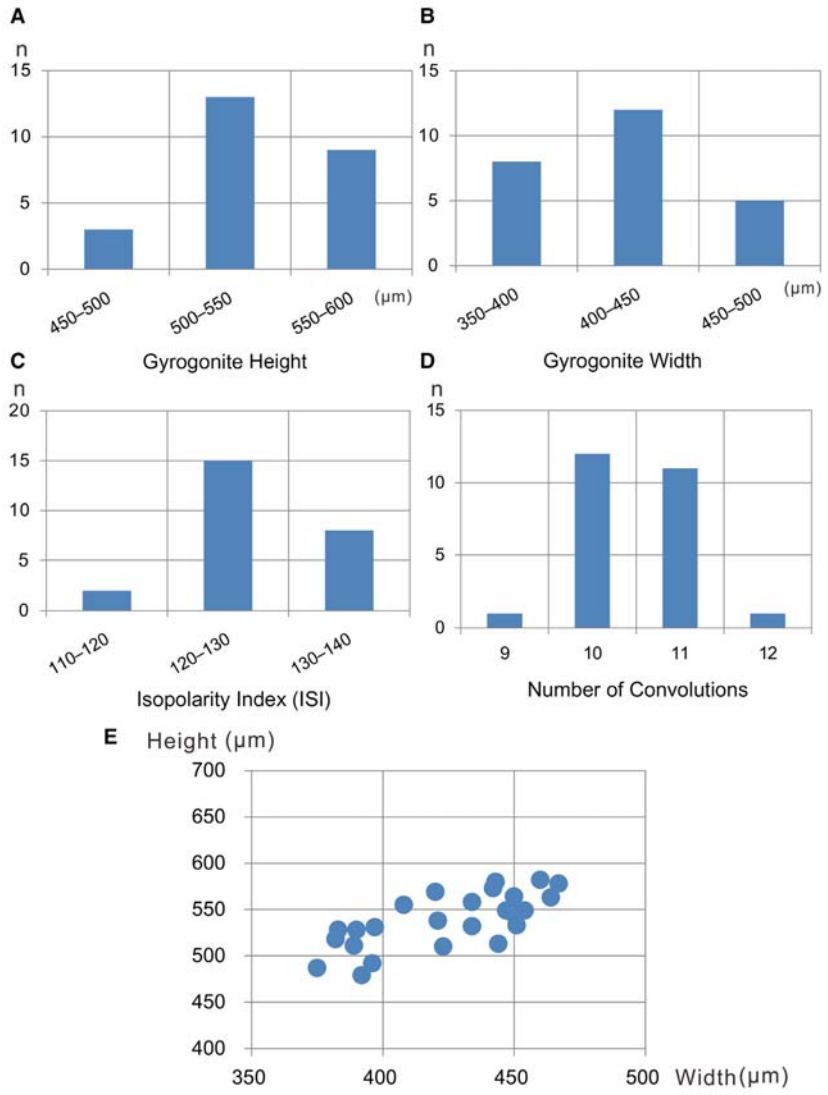

FIG. 17. Biometric data of *Collichara taizhouensis* (25 gyrogonites from the depth of 307.05 m) in the SK-1(North) borehole, Songliao Basin. A, height. B, width. C, isopolarity index (ISI). D, number of convolutions. E, dispersion graph of height/width. Colour online.

isopolarity index ranging from 112 to 147 (often 120–140); 7–8 convolutions are observed in lateral view. Spiral cells are convex, sometimes concave or flat, 120–140 μm wide, occasionally ornamented with a continuous, sometimes wavy mid-cellular crest, parallel to the sutures, accounting for about 30–40% of the width of the spiral cells. In some cases, there is an additional thinner crest below the suture (Fig. 16K). The apex is flat, with well-marked periapical thinning and moderate narrowing of the spiral cells. The central part of the apex shows prominent nodules, generally forming a well-developed rosette. Base is flat and displays a well-marked basal funnel, with a pentagonal basal pore, 55–70 μm in size. Basal plate was not observed in material from the Songliao Basin but has been described as a unicellular pentagonal prism in the North Jiangsu Basin (Wang *et al.* 1982).

Remarks. This species was first assigned to the genus *Neochara*, which was defined by Wang (1978*b*) based on gyrogonites from the Jianghan Basin. In this study, this species is newly combined with *Peckichara* based on its apical features. It cannot be assigned to the genus *Lychnothamnus* (*Stephanochara*) because of the periapical narrowing of the spiral cells. It shows similar apical and basal features as *Nitellopsis*, from which it differs in its shape, a reduced narrowing and its prismatic basal plate (discoidal in *Nitellopsis*).

Distribution. *Peckichara sinuolata* was first described in the upper Paleocene and lower Eocene in the North Jiangsu Basin (Wang *et al.* 1982; Wang 2004). It has also been found in the Nanxiong Basin, Shanghu Formation (Huang 1988).

SEDIMENTOLOGY, TAPHONOMY AND PALAEOECOLOGY

Combined sedimentological and taphonomic analyses were carried out in the SK-1(North) borehole in the

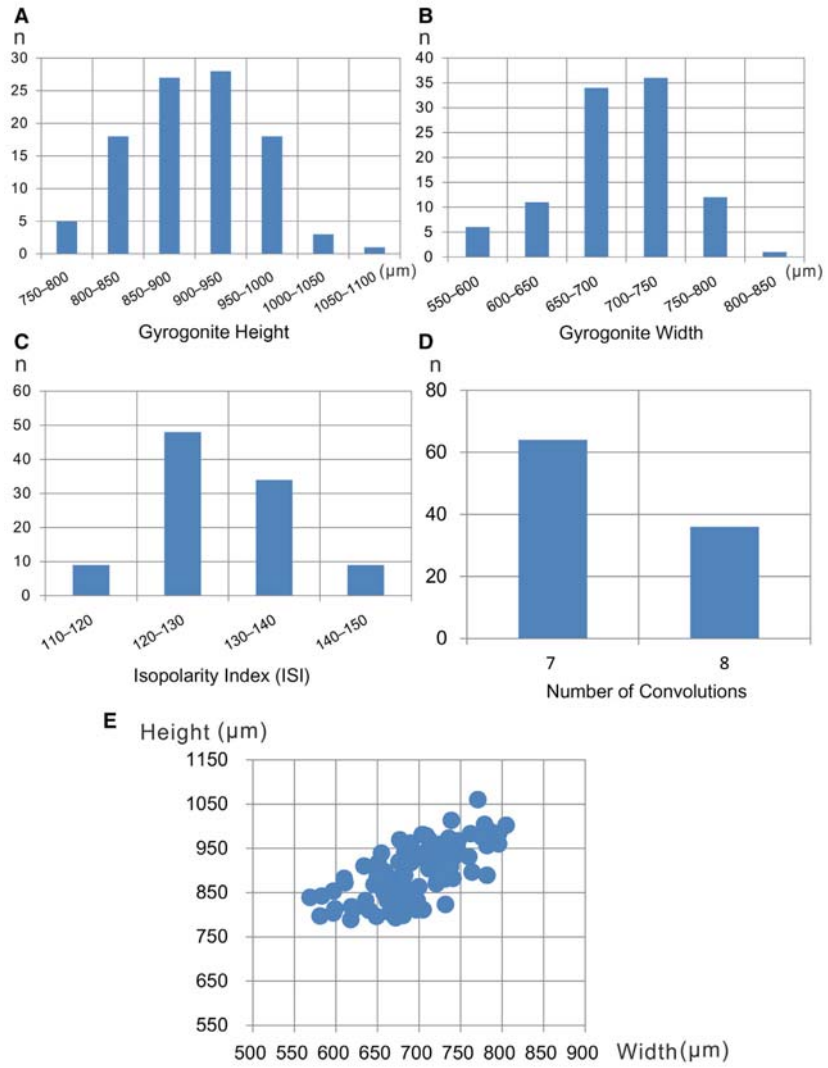

FIG. 18. Biometric data of *Peckichara sinuolata* (100 gyrogonites from the depth of 325.59 m) in the SK-1(North) borehole, Songliao Basin. A, height. B, width. C, isopolarity index (ISI). D, number of convolutions. E, dispersion graph of height/width. Colour online.

Songliao Basin in order to establish the palaeoenvironment of charophyte assemblages and to explore the extent to which they were influenced by palaeoecological changes in their vertical evolution. High resolution continuous sedimentary records have been studied by Cheng *et al.* (2009, 2011) and Wang *et al.* (2015), providing a basis on which to perform our study.

The Sifangtai and Mingshui formations are mainly composed of alternating red and grey siltstones and claystones, indicating lacustrine conditions. Four intervals have been distinguished and are described below, from base to top.

The first interval (1022–807 m in depth) is mainly formed of red, green and grey siltstones and claystones containing calcareous concretions, occasionally interbedded with thin conglomerates and grey sandstones, related to shallow lake and lake shore deposits, the nodules being attributed to the activity of higher plant roots in hydromorphic soils. Conglomerates are generally matrix-supported with clasts composed of sandstones and claystones, up to 6 cm in diameter, poorly sorted, angular to sub-angular in shape, representing debris flows in an alluvial fan context. Charophytes were very abundant in claystones, including *Atopochara trivolvis ulanensis*, *Mesochara biacuta*, *Microchara leiocarpa*, *Lamprothamnium ellipticum* and *Lychnothamnus yuntaishanensis*. Good preservation of these fossils is considered proof of autochthony in shallow lacustrine facies with abundant terrigenous inputs.

The second interval (807–630 m in depth) is mainly composed of grey siltstones and claystones containing calcareous concretions, intercalated with sandstones showing horizontal and planar cross-bedding (Cheng *et al.* 2009, 2011; Wang *et al.* 2015). The fine-grained sediments have been attributed to deeper lake deposits while coarse-grained deposits were attributed to tempestites (Cheng *et al.* 2009, 2011). No charophyte remains were found.

The third interval (630–292 m) consists of red, green, and grey siltstones and claystones with abundant

calcareous concretions, attributed to shallow lacustrine facies with abundant terrigenous inputs. These deposits are occasionally interbedded with grey sandstones and matrix-supported conglomerate beds, 10–30 cm thick, with clasts formed mainly by sandstones and claystones, up to 30 mm in diameter, poorly sorted, angular to subrounded in shape, attributed to debris flows in an alluvial fan context. Charophytes found in claystones included *Sphaerochara parvula*, *S. jacobii*, *Mesochara biacuta*, *Mesochara* aff. *stantoni*, *Microchara gobica*, *M. leiocarpa*, *M. cristata*, *M. prolixa*, *Chara changzhouensis*, *Nemegtichara prima*, *Nodosochara (Turbochara) specialis*, *Lychnothamnus* aff. *vectensis*, *Collichara taizhouensis* and *Peckichara sinuolata*, being well preserved and considered autochthonous in shallow lacustrine facies.

The fourth interval (292–212 m) is mainly composed of grey siltstones and claystones, occasionally interbedded with conglomerates and grey sandstones. This interval is devoid of charophytes and would indicate relatively deeper lacustrine facies in comparison to the previous interval (Cheng *et al*. 2009, 2011; Wang *et al.* 2015).

Based on the above sedimentological and taphonomic observations, the charophyte flora from the Sifangtai and Mingshui formations in the Songliao Basin is considered to represent shallow freshwater lake facies with significant terrigenous inputs. This information is important to highlight that there were no significant palaeoenvironmetal constraints controlling the charophyte succession throughout the borehole studied.

BIOSTRATIGRAPHY

Upper Cretaceous charophyte biostratigraphy has a long tradition in Europe. The first biozonation, composed of three biozones, was proposed by Grambast (1971). Later, a European Cretaceous–Paleocene charophyte biozonation was developed mainly in the south Pyrenean basins (Catalonia, Spain) by Feist & Colombo (1983) and Feist *in* Galbrun *et al*. (1993). Feist *in* Riveline *et al*. (1996) proposed seven charophyte biozones for the Santonian – early Danian interval, in part calibrated to the GPTS through magnetostratigraphy. Recently, Vicente *et al*. (2015, 2016) modified this biozonation and provided a new calibration to the GPTS.

China constitutes another major area where Cretaceous–Paleocene charophyte biostratigraphy has been studied in detail. The most extensively studied basins include the Songliao (Wang *et al.* 1985; Li *et al*. 2013), Junggar (Yang *et al*. 2005, 2008), Pingyi (Zhang *et al*. 2014), North Jiangsu (Wang *et al.* 1982; Wang 2004), Jianghan (Wang 1978*a, b*; Li *et al*. 2010) and Nanxiong (He & Huang 1979; Huang 1988) basins. Recently, Li *et al*. (2016) restudied the charophyte flora from the Pingyi Basin based on modern concepts in charophyte biostratigraphy, taking into account species polymorphism to define species as well as palaeoenvironmental constraints, and established two biozones based on index species with a Eurasiatic range. This enabled a long-distance biostratigraphic correlation between Chinese and European biozonations. These biozones were a latest Campanian – early Danian *Microchara cristata* Zone and a late Danian – earliest Eocene *Peckichara varians* Zone.

The aim of the present study was to revise the charophyte biozones established by Wang *et al.* (1985) in the Songliao Basin on the basis of the same criteria used for the Pingyi Basin. Four biozones included within one superzone were established (Fig. 19). The magnetostratigraphy provided by Deng *et al*. (2013) allowed calibration of the newly created biozonation to the GPTS.

The base of SK-1(North) borehole studied in the Songliao basin, that is, between −1023.22 m and −964.57 m in depth, corresponds to an interval without any significant biostratigraphic marker. The flora is composed of *Mesochara biacuta*, *Microchara leiocarpa* and *Lychnothamnus yuntaishanensis*. This interval is calibrated to the lower part of chron C33n, middle Campanian in age (Deng *et al*. 2013).

Atopochara trivolvis ulanensis *Zone*

Definition. Partial range zone between the FAD (first appearance datum) of *Atopochara trivolvis ulanensis* and the FAD of *Microchara gobica*. Other abundant species in this zone include *Mesochara biacuta*, *Microchara leiocarpa*, *Lamprothamnium ellipticum* and *Lychnothamnus yuntaishanensis*.

Correlation with other biozonations. This partial range zone is equivalent to the *Atopochara ulanensis–Hornichara anguangensis* Assemblage Subzone established by Wang *et al.* (1985) since *Hornichara anguangensis* has been synonymized with *Microchara leiocarpa*.

Calibration to the GPTS. This biozone encompasses charophyte assemblages between −964.57 m and −813.57 m in depth in the SK-1(North) borehore in the Songliao basin and is correlated to chrons C33n to mid–C32n.2n (Deng *et al*.2013).

Age. Late Campanian (latest Campanian not included).

Microchara cristata *Superzone*

A *Microchara cristata* Zone was first proposed by Feist *in* Galbrun *et al*. (1993) in Spain, encompassing three zones

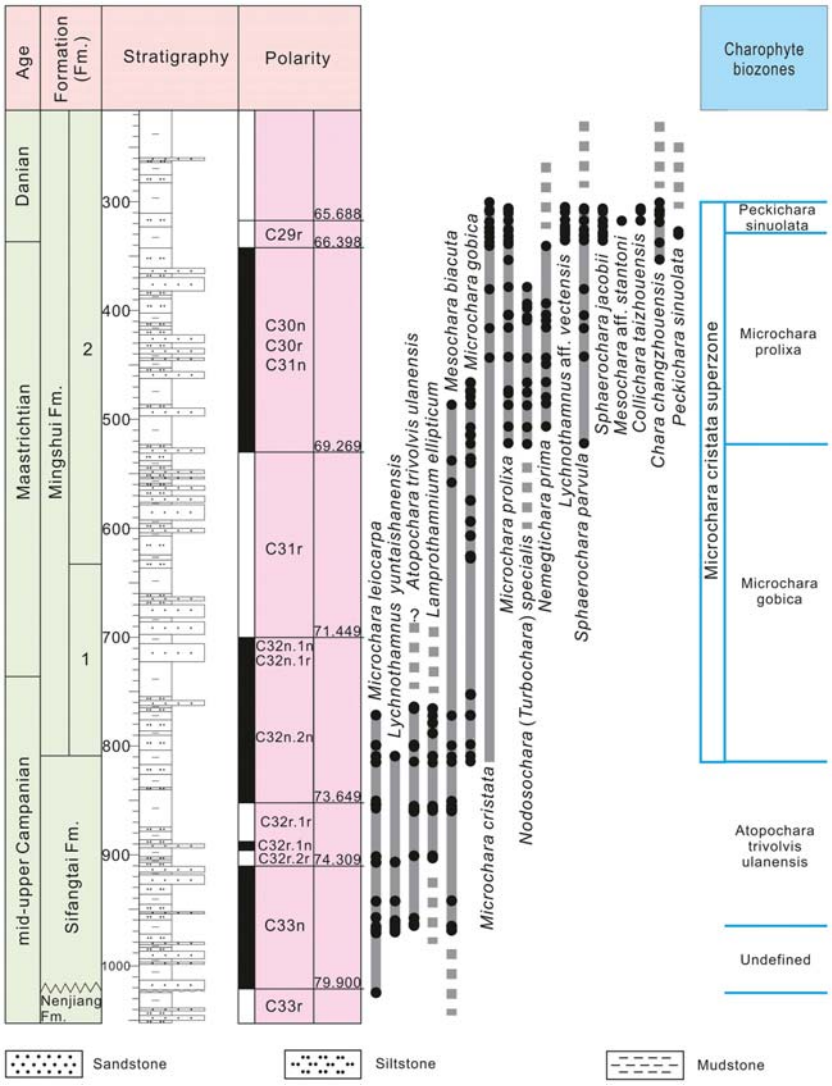

FIG. 19. Stratigraphic log of the SK-1(N) borehole showing position of samples and biostratigraphy of charophytes, calibrated to the GPTS (Deng *et al.* 2013). Colour online.

named as lower, middle and upper *Microchara cristata* zones with the upper zone being further divided into two subzones. In China, the *Microchara cristata* Zone was also used in the Pingyi Basin (Zhang *et al.* 2014; Li *et al.* 2016), where it is defined as the interval between the first occurrence of *Microchara cristata* Grambast and the first occurrence of *Peckichara varians* Grambast. In the Catalan Pyrenees (Spain), the range of this species has been calibrated to magnetozones C32n to C29r (Galbrun *et al.* 1993; Vicente *et al.* 2015), ranging from the latest Campanian to earliest Danian in age.

From a biogeographical viewpoint, *Microchara cristata* is a species of at least Eurasiatic distribution. From a palaeoecological viewpoint, this species tolerated a wide array of habitats, including permanent freshwater lakes, brackish water and floodplain ponds (Vicente *et al.* 2015, 2016), and lacustrine facies within a fluvial context (Li *et al.* 2016). Therefore, this species is useful for large-scale biostratigraphic correlation, and a superzone is proposed in this study, which includes three biozones: the *Microchara gobica*, *Microchara prolixa* and *Peckichara sinuolata* zones.

Microchara gobica *Zone*

Definition. Partial range zone between the FAD of *Microchara gobica* and the FAD of *Microchara prolixa*. Other abundant species in the same biozone include *Atopochara trivolvis ulanensis*, *Mesochara biacuta*, *Microchara leiocarpa*, *Lamprothamnium ellipticum* and *Lychnothamnus yuntaishanensis*.

Comparison with other biozonations. This zone can be compared to the assemblage subzone *Atopochara ulanensis–Latochara longiformis* established by Wang *et al.* (1985). However, *Latochara longiformis* is a poorly defined species, because the apical pore was not visible (Wang *et al.* 1985). The charophyte assemblage described

by Karczewska & Ziembińska-Tworzydło (1981) from the Upper Cretaceous in Mongolia belongs to the *Microchara gobica* Zone due to the occurrence of the index species together with *Atopochara trivolvis ulanensis*, *Mesochara biacuta* and *Lamprothamnium ellipticum*. Here the *M. gobica* Zone is tentatively included within the *M. cristata* Superzone based on the age of *Microchara cristata* in Europe (latest Campanian – early Danian). However, the two species do not co-occur in the Songliao Basin.

Calibration to the GPTS. This zone encompasses charophyte assemblages between −813.57 and −521.71 m in depth in the SK-1(North) borehole in the Songliao basin and is calibrated to chrons mid-C32n.2n to basal C31n (Deng *et al*. 2013).

Age. Latest Campanian – early Maastrichtian.

Microchara prolixa *Zone*

Definition. This zone is defined between the FAD of *Microchara prolixa* and the FAD of *Peckichara sinuolata*. Associated species are *Sphaerochara parvula*, *S. jacobii*, *Mesochara biacuta*, *Microchara gobica*, *M. cristata*, *Chara changzhouensis*, *Nemegtichara prima*, *Nodosochara* (*Turbochara*) *specialis* and *Lychnothamnus* aff. *vectensis*.

Comparison with other biozonations. This zone can be correlated to the *Atopochara ulanensis–Hornichara prolixa* Assemblage Subzone established by Wang *et al.* (1985).

Calibration to the GPTS. This zone encompasses charophyte assemblages between −521.71 and −329.06 m in depth in the SK-1(North) borehole in the Songliao Basin, which are calibrated to the magnetic zones of C31n to the base of C29r (Deng *et al*. 2013).

Age. Late Maastrichtian.

Peckichara sinuolata *Zone*

Definition. The base of this zone is defined by the FAD of *Peckichara sinuolata*. The top is undefined in the Songliao basin due to the lack of a charophyte fossil record in the upper part of the SK-1(North) borehole. This biozone includes a diverse assemblage. Besides *Sphaerochara parvula*, *S. jacobii*, *Chara changzouensis*, *Microchara cristata*, *M. prolixa* and *Lychnothamnus* aff. *vectensis*, which were already present in the underlying deposits, *Mesochara* aff. *stantoni*, *Collichara taizhouensis* and *Peckichara sinuolata* first appear in this biozone.

Calibration to the GPTS. This zone encompasses charophyte assemblages between −329.06 and −299.74 m in depth in the SK-1(North) borehole in the Songliao Basin, which are calibrated to the upper part of chron C29r with an age of 66–65 Ma (Deng *et al*. 2013).

Remarks. Peckichara sinuolata is a widely distributed species in China, reported in the North Jiangsu and Nanxiong basins (Wang *et al.* 1982; Huang 1988; Wang 2004). Therefore, this species is useful for biostratigraphic correlation.

Age. Earliest Danian.

DISCUSSION

The polymorphism of charophyte species from the Songliao Basin has been characterized based on rich gyrogonite populations, and as a result some significant synonymies are proposed. In the twentieth century, charophyte taxonomy from the Songliao Basin was based on studies by the Polish–Mongolian palaeontological expeditions carried out in 1964 and 1965 and subsequently published by Karczewska & Ziembińska-Tworzydło (1969, 1972, 1981, 1983), Kyansep-Romaschkina (1975) and Karczewska & Kyansep-Romaschkina (1979). Indeed, the Songliao and Mongolian basins are palaeogeographically very close to each other. Researchers typically identified charophyte species based on a few gyrogonites, without taking into account the polymorphism of the whole population. This resulted in an inflated taxonomy. For example, *Microchara gobica* included *Raskyaechara gobica*, *Raskyaechara gobica* var. *songliaoensis* and *Raskyaechara costulata* based on differences in general size, or on the width of the mid-cellular crests. One of the goals of the present study was to correct these biases, bringing taxonomic methods into line with those using modern criteria.

Four partial range zones have been defined in the Songliao Basin, a number of which are included within the supracontinental *Microchara cristata* Superzone. All of these biozones were calibrated to the GPTS through magnetostratigraphy. This is the first time that such a calibration has been provided for a Chinese charophyte biozonation. The new biozonation can be applied to other Chinese basins including the Erlian, Junggar, North Jiangsu, Jianghan and Nanxiong basins. For example, *Microchara cristata*, which was also found in the Jianghan Basin, can be used to correlate the biostratigraphy between the two basins. *Peckichara sinuolata* is found in the North Jiangsu and Nanxiong basins and the homonymous biozone can be used for inter-basin correlation.

Furthermore, the new biozonation can be correlated with that of other countries and continents such as Mongolia and Europe. For example, in Mongolia, the age of the *Atopochara trivolvis ulanensis* Zone can be directly applied. The *Microchara cristata* Superzone allows correlation of the Chinese biozonation with current European biozonations, since a group of coeval biozones based on *Microchara cristata* has been proposed by Feist *in* Galbrun *et al.* (1993) for the Pyrenees.

The palaeoecological study developed here provides important data to compare the charophyte floras from the Songliao and Pingyi basins. During the latest Campanian and Maastrichtian, *Microchara cristata* and *Lamprothamnium ellipticum* were found in the freshwater deposits of the Songliao and Pingyi basins. However, in the Pingyi Basin, *Feistiella anluensis* was abundant in brackish facies, whereas this species is completely absent in Songliao, where only freshwater facies occur. In the Paleocene Songliao Basin, a diverse flora consisting of *Sphaerochara parvula*, *S. jacobii*, *Mesochara* aff. *stantoni*, *Microchara cristata*, *M. prolixa*, *Lychnothamnus* aff. *vectensis*, *Collichara taizhouensis*, *Chara changzhouensis* and *Peckichara sinuolata* thrived in lacustrine settings with terrigenous inputs, whereas the flora in the Pingyi Basin was monotonously dominated by *Peckichara varians* inhabiting permanent and alkaline lake environments. *Sphaerochara parvula* was found in both basins, indicating that it had fewer ecological constraints.

In the Late Cretaceous, *Atopochara trivolvis ulanensis* was only found in the Songliao Basin and adjacent areas such as Inner Mongolia and Mongolia (Kyansep-Romaschkina 1975; Van Itterbeeck *et al.* 2005). However, this species does not occur in the southern basins of China, or elsewhere, suggesting that during the Maastrichtian it was endemic to northern China and Mongolia, and subject to strong latitudinal control (Martín-Closas & Wang 2008).

From an evolutionary point of view, there are two critical turnovers in the charophyte floras from the Songliao basin. In the mid-Maastrichtian, *M. prolixa* and *Nemegtichara prima* first appeared. This event is coeval with the mid-Maastrichtian Event, with an abrupt reorganization of oceanic circulation and the first Late Cretaceous wave of marine plankton extinctions (Frank & Arthur 1999; Keller 2001). This event probably meant fluctuating warming on the continent during this period (Li & Keller 1998). The end-Cretaceous crisis represents the second species turnover and shows a clear floral diversification at the middle part of chron C29r, when three species appeared quite suddenly: *Mesochara* aff. *stantoni*, *Collichara taizhouensis* and *Peckichara sinuolata*. Based on last occurrences of taxa, the extinction pattern is gradual and extended to chrons C30n and C29r. Most of these Paleocene species are also common in other Chinese basins such as the North Jiangsu Basin and the Nanxiong Basin (Wang 2004; Huang 1988).

CONCLUSIONS

In the Songliao Basin, the middle Campanian – Maastrichtian charophyte flora is composed of up to 14 species: *Atopochara trivolvis ulanensis*, *Sphaerochara parvula*, *S. jacobii*, *Mesochara biacuta*, *Microchara gobica*, *M. cristata*, *M. leiocarpa*, *M. prolixa*, *Chara changzhouensis*, *Nemegtichara prima*, *Lamprothamnium ellipticum*, *Nodosochara* (*Turbochara*) *specialis*, *Lychnothamnus yuntaishanensis* and *L.* aff. *vectensis*. The Paleocene flora consists of nine species. Besides *S. parvula*, *S. jacobii*, *Chara changzhouensis*, *Microchara cristata*, *M. prolixa* and *L.* aff. *vectensis*, which were already present in the underlying deposits, there are three newly appeared species: *Mesochara* aff. *stantoni*, *Collichara taizhouensis* and *Peckichara sinuolata*. These floras contain endemic, latitudinally distributed elements, such as *Atopochara trivolvis ulanensis*, along with other species that show a Eurasiatic distribution, such as *Microchara cristata*.

The biozonation proposed here consists of four biozones, three of them belonging to one superzone (the *Microchara cristata* Superzone). All of them are well calibrated to the GPTS through magnetostratigraphy. These biozones are the *Atopochara trivolvis ulanensis* Zone (late but not latest Campanian), the *Microchara gobica* Zone (latest Campanian – early Maastrichtian), the *Microchara prolixa* Zone (late Maastrichtian) and the *Peckichara sinuolata* Zone (earliest Danian).

The Songliao Basin charophyte flora is most similar to that of the neighbouring Nemegt Basin in Mongolia, with *Atopochara trivolvis ulanensis*, *Sphaerochara jacobii*, *Mesochara biacuta*, *Microchara gobica*, *M. cristata* and *Nemegtichara prima* being found in both basins. The Songliao and Pingyi basins also share some species, including *Sphaerochara parvula*, *Microchara cristata* and *Lamprothamnium ellipticum*. Furthermore, floras of the Songliao Basin and the coeval European basins can also be correlated through the *Microchara cristata* Superzone.

Further improvements are required to the Chinese charophyte biostratigraphy of the Campanian and Paleocene. Palaeoecological studies applied to other Chinese basins will help to gain a better understanding of the influence of facies on the distribution of charophyte species. In addition, palaeobiogeographical constraints require further study to improve correlations between northern and southern Chinese basins based on charophyte biostratigraphy.

Acknowledgements. This study is a contribution to projects CGL2015-69805-P, funded by the Spanish Ministry of Economy

and Competitiveness (MINECO) and the European Fund for Regional Development (EFRD), project 2017SGR-824 from the Catalan Research Agency (AGAUR), project grant nos. 41688103, 41602003, funded by the National Natural Science Foundation of China and Strategic Priority Pre-Research Program (B) of the Chinese Academy of Sciences (XDPB05). Weimin Si, Haiying Qu, Manyan Wang, Lijun Deng, Yujie Tu and Tian Jiang from China University of Geosciences, Beijing and Ming Shi and Yu Zhang helped us greatly to prepare samples and pick out fossils. Huinan Lu (Nanjing Institute of Geology and Palaeontology, CAS) and Josep Sanjuan (American University of Beirut) are acknowledged for discussion of the systematic palaeontology of fossils. We are grateful to the Editor in Chief of *Papers in Palaeontology*, Andrew Smith, Sally Thomas and to the reviewers Ingeborg Soulié-Märsche (Université de Montpellier) and Josep Sanjuan (American University of Beirut) for their constructive criticism during the peer-review process. The English text was corrected by Denise Phelps (University of Barcelona).

Editor. Andrew Smith

REFERENCES

AGARDH, C. A. 1824. *System Algarum*. Lundæ, Literis Berlingianis, 312 pp.

BRAUN, A. and NORDSTEDT, C. F. O. 1882. *Fragmente einer Monographie der Characeen*. Königlichen Akademie der Wissenschaften, Berlin, 211 pp.

CANDE, S. C. and KENT, D. V. 1995. Revised calibration of the geomagnetic polarity timescale for the Late Cretaceous and Cenozoic. *Journal of Geophysical Research: Solid Earth*, **100**, 6093–6095.

CHENG, R. H., WANG, G. D., WANG, P. J. and GAO, Y. F. 2009. Uppermost Cretaceous sediments: sedimentary microfacies and sedimentary environment evolution of Sifangtai Formation and Mingshui Formation in SK-I(n). *Earth Science Frontiers*, **16**, 85–95. [in Chinese, English abstract]

—— —— —— —— REN, Y. G., WANG, C. S., ZHANG, S. H. and WANG, Q. Y. 2011. Centimeter-scale sedimentary sequence description of Upper Cretaceous–Lower Paleocene Mingshui Formation: lithostratigraphy, facies and cyclostratigraphy, based on the scientific drilling (SK1) borehole in the Songliao Basin. *Earth Science Frontiers*, **18**, 285–328. [in Chinese, English abstract]

DENG, C. L., HE, H. Y., PAN, Y. X. and ZHU, R. X. 2013. Chronology of the terrestrial Upper Cretaceous in the Songliao Basin, northeast Asia. *Palaeogeography, Palaeoclimatology, Palaeoecology*, **385**, 44–54.

FEIST, M. and COLOMBO, F. 1983. La limite Crétacé-Tertiaire dans le nord-est de l'Espagne, du point de vue des charophytes. *Géologie Méditerranéenne*, **10**, 303–326.

—— and FREYTET, P. 1983. Conséquences stratigraphiques de la répartition des charophytes dans le Campanien et le Maastrichtien du Languedoc. *Géologie Méditerranéenne*, **10**, 291–301.

—— GRAMBAST-FESSARD, N., GUESQUERLIN, M., KAROL, K., LU, H. N., McCOURT, R., WANG, Q. F. and ZANG, S. Z. 2005. *Treatise on invertebrate paleontology. Part B. Protoctista 1. Volume 1. Charophyta*. Geological Society of America & University of Kansas Press, 170 pp.

FENG, Z. Q., JIA, C. Z., XIE, X. N., ZHANG, S., FENG, Z. H. and CROSS, T. A. 2010. Tectonostratigraphic units and stratigraphic sequences of the nonmarine Songliao basin, northeast China. *Basin Research*, **22**, 79–95.

FRANK, T. D. and ARTHUR, M. A. 1999. Tectonic forcings of Maastrichtian ocean-climate evolution. *Paleoceanography*, **14**, 103–117.

GALBRUN, B., FEIST, M., COLOMBO, F., ROCCHIA, R. and TAMBAREAU, Y. 1993. Magnetostratigraphy and biostratigraphy of Cretaceous-Tertiary continental deposits, Ager basin, province of Lerida, Spain. *Palaeogeography, Palaeoclimatology, Palaeoecology*, **102**, 41–52.

GAO, R. Q., ZHANG, Y. and CUI, T. C. 1994. *Cretaceous petroleum bearing strata in the Songliao Basin*. The Petroleum Industry Press, Beijing, 333 pp. [in Chinese, English abstract]

GAO, Y., WANG, C., LIU, Z., ZHAO, B. and ZHANG, X. 2013. Clay mineralogy of the middle Mingshui Formation (upper Campanian to lower Maastrichtian) from the SKIn borehole in the Songliao Basin, NE China: implications for palaeoclimate and provenance. *Palaeogeography, Palaeoclimatology, Palaeoecology*, **385**, 162–170.

GRADSTEIN, F. M., OGG, J. G. and SMITH, A. G. 2004. *A geologic time scale 2004*. Cambridge University Press, 589 pp.

GRAMBAST, L. 1957. Ornementation de la gyrogonite et systématique chez les Charophytes fossiles. *Revue Générale de Botanique*, **64**, 339–362.

—— 1958. Etude sur les charophytes tertiaires d'Europe Occidentale et leurs rapports avec les formes actuelles. PhD thesis, Paris University, 258 pp.

—— 1959. *Extension chronologique des genres chez les Charoideae*. Société des éditions Technip, Paris, 12 pp.

—— 1962. Classification de l'embranchement des Charophytes. *Naturalia Monspeliensia (Série Botanique)*, **14**, 63–86.

—— 1967. La série évolutive *Perimneste-Atopochara* (charophytes). *Comptes Rendus des Séances de L'Académie des Sciences Paris*, **264**, 581–584.

—— 1968. Evolution of the utricle in the charophyte genera *Perimneste* Harris and *Atopochara* Peck. *Journal of the Linnean Society of London (Botany)*, **61**, 5–11.

—— 1971. Remarques phylogénétiques et biochronologiques sur les Septorella du Crétacé terminal de Provence et les Charophytes associcées. *Paléobiologie Continentale*, **2**, 1–38.

—— and GUTIÉRREZ, G. 1977. Espèces nouvelles de charophytes du Crétacé supérieur terminal de la province de Cuenca (Espagne). *Paléobiologie Continentale*, **8**, 1–34.

GROVES, J. 1916. On the name *Lamprothamnus* Braun. *Journal of Botany*, **54**, 336–337.

—— 1926. Charophyta. 165–173. *In* REID, E. M. and CHANDLER, M. E. J. (eds), *The Bembridge flora*. British Museum Catalogue, Cainozoicum Plants, London.

HAO, Y. C., RUAN, P. H., ZHOU, X. G., SONG, Q. S., YANG, G. D., CHENG, S. W. and WEI, Z. X. 1983. Middle Jurassic–Tertiary Deposits and Ostracod and Charophyte fossil assemblages in the Xining and Minhe Basins. *Earth Science: Journal of Wuhan Geology College*, **23**, 1–210.